

AD-A128 069

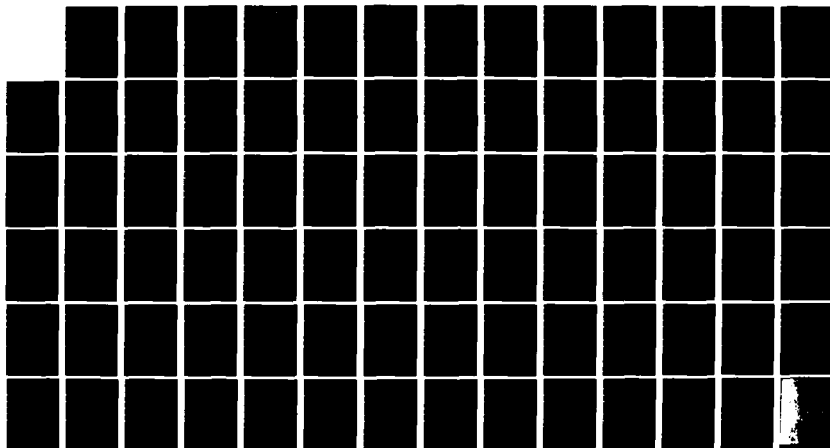
MONTE CARLO CALCULATIONS OF MASS SPECTROMETER FLOW(U)  
SPECTRAL SCIENCES INC BURLINGTON MA J B ELGIN FEB 83  
SSI-TR-30 AFGL-TR-83-0057 F19628-82-C-0048

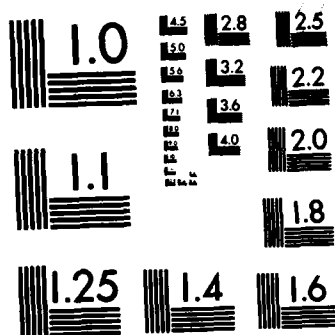
1/1

UNCLASSIFIED

F/G 7/4

NL





MICROCOPY RESOLUTION TEST CHART  
NATIONAL BUREAU OF STANDARDS-1963-A

AFGL-TR-83-0057

MONTE CARLO CALCULATIONS OF  
MASS SPECTROMETER FLOW

James B. Elgin

Spectral Sciences, Inc.  
99 So. Bedford Street  
Burlington, MA 01803

Scientific Report No. 1

February 1983

Approved for public release; distribution unlimited

AIR FORCE GEOPHYSICS LABORATORY  
AIR FORCE SYSTEMS COMMAND  
UNITED STATES AIR FORCE  
HANSOM AFB, MASSACHUSETTS 01731

DTIC  
SELECTE  
MAY 10 1983  
H

83 05 10 003

DTIC FILE COPY

AD A 128069

Qualified requestors may obtain additional copies from the Defense Technical Information Center. All others should apply to the National Technical Information Service.

UNCLASSIFIED

SECURITY CLASSIFICATION OF THIS PAGE (When Data Entered)

REPORT DOCUMENTATION PAGE		READ INSTRUCTIONS BEFORE COMPLETING FORM
1. REPORT NUMBER AFGL-TR-83-0057	2. GOVT ACCESSION NO. A128 069	3. RECIPIENT'S CATALOG NUMBER
4. TITLE (and Subtitle)  MONTE CARLO CALCULATIONS OF MASS SPECTROMETER FLOW		5. TYPE OF REPORT & PERIOD COVERED Scientific Report No. 1 26 Jan. 82 - 26 Jan. 83
7. AUTHOR(s)  James B. Elgin		6. PERFORMING ORG. REPORT NUMBER SSI-TR-30
8. PERFORMING ORGANIZATION NAME AND ADDRESS Spectral Sciences, Inc. 99 So. Bedford Street Burlington, MA 01803		6. CONTRACT OR GRANT NUMBER(s)  F19628-82-C-0048
9. CONTROLLING OFFICE NAME AND ADDRESS Air Force Geophysics Laboratory Hanscom AFB, Massachusetts 01731 Monitor/Christopher Sherman/LKD		10. PROGRAM ELEMENT, PROJECT, TASK AREA & WORK UNIT NUMBERS 62101F 668703AQ
11. MONITORING AGENCY NAME & ADDRESS (if different from Controlling Office)		12. REPORT DATE February 1983
		13. NUMBER OF PAGES 80
		14. SECURITY CLASS. (of this report) UNCLASSIFIED
		15. DECLASSIFICATION/DOWNGRADING SCHEDULE
16. DISTRIBUTION STATEMENT (of this Report)  Approved for public release; distribution unlimited.		
17. DISTRIBUTION STATEMENT (of the abstract entered in Block 20, if different from Report)		
18. SUPPLEMENTARY NOTES		
19. KEY WORDS (Continue on reverse side if necessary and identify by block number)  Mass Spectrometer                      Monte Carlo Flowfield Freejet Expansion                      Ionic Sampling		
20. ABSTRACT (Continue on reverse side if necessary and identify by block number)  The initial phase of research to develop a Monte Carlo description of the flow within an ionic sampling mass spectrometer. Procedures for handling multiple species, chemical reactions and internal energy transfer are discussed at length. The flow through a sonic orifice for major species is computed and methods for handling minor species are presented.		

DD FORM 1 JAN 73 1473

EDITION OF 1 NOV 65 IS OBSOLETE  
S/N 0102-10-014-6401

UNCLASSIFIED

SECURITY CLASSIFICATION OF THIS PAGE (When Data Entered)

# CONTENTS



Accession For  
NTIS GRA&I  
DTIC Tab  
Unannounced  
Justification

By  
Distribution/  
Availability Codes  
Avail and/or  
Special

1  
A

ABSTRACT .....	1
1. INTRODUCTION .....	6
1.1 Project Description .....	6
1.2 Overview of the Direct Simulation Monte Carlo Method .....	7
2. GAS MODEL AND EQUILIBRIUM PROPERTIES .....	8
2.1 Preliminary Equilibrium Gas Relations .....	8
2.2 Analytical Form of The Collision Cross Section .....	10
2.3 Equilibrium Reference Properties for a Multi-Component Gas .....	13
2.4 Internal Energy Model .....	15
3. INTERNAL REPRESENTATION .....	16
3.1 State Vector .....	16
3.2 Reduction to a Reasonable Number of Simulated Molecules .....	17
3.3 Internal Scales .....	17
3.4 Weighting Factors .....	19
4. COLLISION MECHANICS .....	21
4.1 Relations for Elastic Collisions .....	21
4.2 Simulation of Inelastic Collisions .....	23
4.3 Collisions for Molecules with Distinct Weighting Factors .....	26
4.4 Reactive Collisions .....	27
4.5 Post-Reaction State Definition .....	29
4.6 Dissociative Reactions .....	30
5. MOLECULAR TRANSLATIONS .....	31
5.1 Translation in an Axisymmetric Coordinate System .....	31
5.2 Molecular Cloning .....	33
6. COLLISION SAMPLING IN A MULTI-COMPONENT VHS GAS ...	36
6.1 General Considerations and Approach .....	36
6.2 Collision Sampling for a Single Component Gas.	36
6.2.1 Collision Pair Selection .....	37
6.2.2 Collision Time Counter for a Single Component Gas .....	38

## Contents (Continued)

6.3	Collision Class Sampling in Gas Mixtures .....	41
6.4	Global Collision Sampling in a Gas Mixture ...	42
6.4.1	Global Collision Time Counter .....	42
6.4.2	Collision Pair Selection in Multi- Component Mixtures .....	44
6.4.3	Summary of Collision Sampling in Multi- Component Mixtures .....	45
7.	INITIAL AND BOUNDARY CONDITIONS .....	46
7.1	General Considerations .....	46
7.2	Initial Conditions .....	47
7.2.1	Number of Simulated Molecules and Weighting Factors .....	47
7.2.2	Initial Positions .....	48
7.2.3	Initial Velocity Components .....	49
7.2.4	Initial Internal Energies .....	50
7.3	Wall Boundary Conditions .....	52
7.4	Free Gas Boundary Conditions .....	52
7.4.1	Incoming Number Flux .....	53
7.4.2	Incoming Molecular Velocity Components.	53
7.4.3	Incoming Molecular Position .....	54
7.4.4	Incoming Molecular Internal Energies ..	54
8.	STATISTICAL SAMPLING OF OUTPUT .....	55
8.1	General Considerations .....	55
8.2	Sampling of Instantaneous Output Quantities ..	56
8.3	Sampling of Time Averaged Quantities .....	59
9.	APPLICATION TO THE FREEJET EXPANSION WITHIN A MASS SPECTROMETER .....	60
9.1	Motivation for Studying Major Species Freejet.	60
9.2	Physical Description of the Freejet Expansion.	61
9.3	Potential Computational Approaches .....	64
9.4	Cell Mesh Selection .....	66
9.5	Sample Computational Results .....	69
9.6	Discussion of Freejet Calculations .....	71
9.7	Real Orifice Flow Effects .....	72
9.8	Handling of Minor Species .....	75
9.8.1	Time Counter for Collisions Between Two Minor Species .....	76
9.8.2	Time Counter for Collisions Between Major and Minor Species .....	77
	REFERENCES .....	79

## ILLUSTRATIONS

1. Schematic Showing the Major Features and Flow Regions Involved in The Expansion of a Gas Through a Sonic Orifice Into a Near Vacuum ..... 62
2. Contours of Mach Number and Continuum Breakdown Criterion in the Freejet Expansion of a Diatomic Gas ..... 66
3. A Drawing of a Cell Mesh of the Type Devised for the Initial Freejet Calculations ..... 68
4. Total Axial Number Density as Calculated for a Coarse and a Fine Cell Mesh ..... 70
5. The Discharge Coefficient for a Sharp Edged Orifice as Measured by Smetana, Sherrill and Schort(3) ..... 74



## 1. INTRODUCTION

### 1.1 Project Description

This is the First Yearly Technical Report on a three year effort to study physical processes of relevance to the mass spectrometric measurement of stratospheric ions. The effort involves the development of a Monte Carlo model of the freejet expansion occurring within the mass spectrometer including the effects of agglomeration onto, and fragmentation of, ionic clusters.

The attempt to carry out in situ mass spectrometry in the stratosphere is complicated by changes that may occur in the gas stream as it expands after passage through the orifice. Both positive and negative ions exist in the stratosphere with clustered polar molecules surrounding the ion core. As these ion clusters are carried along in the expanding gas stream, the falling temperature will tend to favor the formation of larger clusters. The charge-dipole interaction is characterized by large cross sections, so agglomeration of polar molecules may change the cluster size distribution that the quadrupole sees from the distribution that exists in the undisturbed stratosphere. Conversely, the measured cluster size distribution may be driven towards smaller clusters via fragmentation. As the ionic clusters are selectively accelerated by the electric field within the mass spectrometer, high energy collisions with neutrals may break apart the clusters.

The present effort involves a Monte Carlo simulation of these processes, so that a model can be used to relate the measured properties to those existing in the undisturbed atmosphere. Sections 2 through 8 describe the method in

general terms, although most of the new results were in fact accomplished in support of the present contract. Section 9 describes particular results obtained when the procedures were applied to the freejet expansion within a mass spectrometer.

## 1.2 Overview of the Direct Simulation Monte Carlo Method

The direct simulation Monte Carlo method, as pioneered by G. A. Bird,<sup>1</sup> provides a powerful technique for the simulation of real gas flows. It bridges the gap between continuum and free molecular flow, retaining validity in either extreme. It can be used to describe complex mixtures, including effects of chemical reactions, heat conduction, viscosity and diffusion for flows in three dimensions. To date, it is the only approach which can demonstrate these abilities for general flow configurations.

The basic calculational technique is well described by its originator in Reference 1, to which frequent reference will be made. The present purpose is to describe how the technique is implemented at Spectral Sciences, Inc. (SSI), with special emphasis on extensions developed at SSI and elsewhere after the publication of Reference 1. Elementary concepts and relations which are essential to a coherent explanation are included here for clarity.

The direct simulation Monte Carlo method involves storing a discrete number of molecules (via their velocities, positions and other pertinent information) in a computer. The solution

---

<sup>1</sup>Bird, G. A., Molecular Gas Dynamics, Clarendon Press, Oxford, 1976.

region is broken up into a number of separate cells, and the solution is stepped forward in time in a two stage process. First, the molecules are advanced along their trajectories by an amount appropriate to their velocity and a time increment  $\Delta t_m$ . In this first stage some molecules will leave the solution region and some will be introduced as determined by the boundary conditions for a particular problem. The second stage is to simulate collisions in each cell appropriate to  $\Delta t_m$  so that collision frequencies are properly simulated. A basic hypothesis of the method is that if the time step is made small enough the processes of translations and collisions can be uncoupled in this manner.

Periodically, the solution is sampled by accumulating statistical sums of number densities, velocities and other basic properties. The solution is run repeatedly until statistical deviations are reduced to a desired limit, and then physically meaningful output quantities are computed from the statistical sums. The number of molecules represented is typically a few thousand at a time, which is vastly fewer than the number of molecules occurring in virtually all real flows. Hence, the construction of a dynamically similar flow to be simulated in the computer is an essential feature of the method.

## 2. GAS MODEL AND EQUILIBRIUM PROPERTIES

### 2.1 Preliminary Equilibrium Gas Relations

For most problems of interest there is a far field equilibrium state whose properties are of relevance to the problem to be solved. Frequently length and velocity scales for the problem are obtained from the far field state and used to

nondimensionalize the internal code variables. Even when the far field state is not used for scaling purposes, it still provides an important comparison case.

For a rest gas in equilibrium the normalized distribution function for the relative speed,  $c_r$ , between molecules of species  $i$  and molecules of species  $j$  is given by<sup>2</sup>

$$f_{ij}(c_r) = \frac{4a_{ij}^{3/2}}{\sqrt{\pi}} c_r^2 \exp(-a_{ij}c_r^2) \quad , \quad (1)$$

where

$$a_{ij} = \frac{\mu_{ij}}{2R_0T_\infty} \quad , \quad (2)$$

and  $\mu_{ij}$  is the reduced mass of the pair; i.e.,

$$\mu_{ij} = \frac{m_i m_j}{m_i + m_j} \quad , \quad (3)$$

with  $m_i$  and  $m_j$  representing the masses of the two species. In these relations,  $T_\infty$  is the far field temperature and  $R_0$  is the universal gas constant. ( $R_0$  is used instead of Boltzmann's constant since the molecular masses will be consistently represented in atomic mass units rather than grams.) The available translational collision energy between two molecules,  $E_c$ , is given by

$$E_c = \frac{1}{2} \mu_{ij} c_r^2 \quad (4)$$

<sup>2</sup>Chapman, Sydney, and Cowling, T. G., The Mathematical Theory of Non-Uniform Gases, 3rd ed. Cambridge University Press, Cambridge, 1970, pp. 6-7.

## 2.2 Analytical Form of The Collision Cross Section

Whenever the direct simulation Monte Carlo method is applied, it is necessary to make tradeoffs between accuracy and simplicity in molecular models. It does no good to use a complex molecular potential surface and then find that reasonable computer run times result in very large statistical fluctuations in the output. Since the final output will reflect errors in the statistics as well as errors in the models, there is a strong impetus to use models which contain the essential physics, but which can be applied in a computationally efficient manner. The current state-of-the-art is the Variable-Hard-Sphere (VHS) model.<sup>3</sup> In this model molecules have a collision cross section which varies as an inverse power of the available collision energy. Hence, if  $\sigma_{ij}$  is the collision cross section for collisions of species  $i$  with species  $j$ , then  $\sigma_{ij}$  is given by a relation of the form

$$\sigma_{ij} = A_{ij} E_c^{-\omega}, \quad (5)$$

where  $A_{ij}$  is a constant coefficient. It follows that the effective diameter for molecules of species  $i$ ,  $d_i$ , is implicitly defined as a function of available collision energy by the relation

$$\sigma_{ii} = \pi d_i^2 = A_{ii} E_c^{-\omega}. \quad (6)$$

$A_{ii}$  can be determined from a reference cross section and velocity via

---

<sup>3</sup>Bird, G. A., "Monte-Carlo Simulation in an Engineering Context," Proceedings of the 12th International Symposium on Rarefied Gas Dynamics, Vol. 74, Progress in Astronautics and Aeronautics, AIAA, New York, 1981.

$$A_{ii} = \left[ \sigma_{ii} (m_i c_r^2 / 4)^\omega \right]_{\text{ref}} \quad (7)$$

If a reference cross section is given for a reference temperature rather than a reference velocity, then the usual choice for the reference velocity is that velocity which has a collision energy equal to the mean collision energy occurring in collisions at the reference temperature. Mathematically, this is equivalent to

$$\left( c_r^2 \right)_{\text{ref}} = \frac{\overline{c_r^3 \sigma_{ii}}}{\overline{c_r \sigma_{ii}}} \quad (8)$$

where the bars over the quantities indicate averages taken over the distribution function given in Eq. (1) evaluated for  $m_i = m_j$  and  $T_\infty = T_{\text{ref}}$ . Equation (8) can be simplified to give

$$\left( c_r^2 \right)_{\text{ref}} = \frac{4(2 - \omega) R_0 T_{\text{ref}}}{m_i} \quad (9)$$

For simulations involving a large number of species, reference cross sections are frequently not available for all possible collision pairs. In this case it is possible to specify  $A_{ii}$  for self collisions only, and then use Eq. (6) to get a molecular diameter as a function of collision energy. Then, applying the relation

$$\sigma_{ij} = \pi \left[ (d_i + d_j) / 2 \right]^2 \quad (10)$$

the coefficient in Eq. (5) for interspecie collisions is given by

$$A_{ij} = \left[ \frac{1}{2} \left( \sqrt{A_{ii}} + \sqrt{A_{jj}} \right) \right]^2 \quad (11)$$

For the internal workings of a Monte Carlo code, it is usually more convenient to express the collision cross section as a function of the relative collision velocity rather than the collision energy. This is simply achieved via the relation

$$\sigma_{ij} = B_{ij} c_r^{-2\omega} , \quad (12)$$

where

$$B_{ij} = A_{ij} \left( \frac{\mu_{ij}}{2} \right)^{-\omega} . \quad (13)$$

The parameter  $\omega$  can be related to  $\eta$ , the exponent of distance in an inverse power intermolecular force law via the relation<sup>3</sup>

$$\omega = 2/(\eta - 1) . \quad (14)$$

Hence, hard sphere molecules (for which  $\eta$  goes to infinity) are represented by  $\omega$  equal to zero. There is a substantial body of evidence, however, that the effective size of molecules does indeed decrease with increasing collision energy, so a positive value of  $\omega$  is usually a better choice.  $\omega$  can be determined from molecular beam data, or from its macroscopic implications. For example, if  $s$  is the temperature exponent for the coefficient of viscosity, then it can be shown<sup>3</sup> that

$$s = \omega + 1/2 , \quad (15)$$

so a measurement of the temperature dependence of the viscosity coefficient serves as an indirect determination of  $\omega$ .

In order to incorporate the model for internal energy transfer to be discussed in Section 4, it is necessary that  $\omega$  be assumed the same for all interactions. This represents one of the major restrictions in the current state of modeling.

Although the sizes of molecules are allowed to vary in the VHS molecular model in deciding whether or not a collision is to occur, when a collision does occur the post collision velocity components are computed as if it were a hard sphere collision (see Section 4). This results in a substantial computational simplification and yet retains good agreement with the macroscopic predictions of the more exact model.<sup>3</sup> (See Reference 1 for a discussion of molecular scattering for general power law potentials.)

### 2.3 Equilibrium Reference Properties for a Multi-Component Gas

One advantage of the VHS model is that the molecules have a well defined cross section, so it is possible to define a mean free path without putting limitations on the minimum deflection angle that is considered. As is the general case for multi-component gases, however, each component has its own mean free path, and the overall mean free path for the mixture must be defined as a weighted average of the mean free paths of the individual species. The somewhat cumbersome relations required to calculate the overall mean free path are given here. It should be noted that the mean free path is calculated only once for a given problem, so the computational effort required to evaluate it is completely negligible.

An individual molecule of species  $i$  will suffer collisions with molecules of species  $j$  with a frequency  $\nu_i^j$  given by

$$\nu_i^j = n_{j\infty} \overline{\sigma_{ij} c_r} \quad (16)$$

where  $n_{j\infty}$  is the number density of species  $j$  and  $\overline{\sigma_{ij} c_r}$  is the average product of cross section times relative velocity for the two species, obtained by integrating over the distribution function given in Eq. (1). When this operation is performed, the result is



$$v_i^j = \frac{2n_{ij}}{\pi} \Gamma(2 - \omega) a_{ij}^{\omega - 1/2}, \quad (17)$$

where  $\Gamma$  denotes the gamma function.

The total collision frequency for an individual molecule of species  $i$ ,  $v_i$ , is obtained by summing Eq. (15) over all species, i.e.

$$v_i = \sum_{j=1}^p v_i^j \quad (18)$$

and the mean free path,  $\lambda_i$ , for molecules of species  $i$  is given by

$$\lambda_i = \bar{c}_i / v_i = \sqrt{\frac{8R_0 T_\infty}{\pi m_i}} / v_i, \quad (19)$$

where  $\bar{c}_i$  is the mean molecular speed for species  $i$  molecules. The mean free path for the gas mixture,  $\lambda_\infty$ , is then defined as the number density weighted average of the  $\lambda_i$  via

$$\lambda_\infty = \sum_{i=1}^p \frac{n_{i\infty} \lambda_i}{n_\infty}, \quad (20)$$

where  $n_\infty$  is the total number density:

$$n_\infty = \sum_{i=1}^p n_{i\infty}. \quad (21)$$

A useful velocity scale is given by  $v_s$ , defined by

$$v_s = \sqrt{\frac{2R_0 T_\infty}{\bar{m}}}, \quad (22)$$

where  $\bar{m}$  is the reference mean molecular weight, i.e.

$$\bar{m} = \sum_{i=1}^p \frac{n_{i\infty} m_i}{n_{\infty}} . \quad (23)$$

$v_g$  is the most probable molecular speed for molecules of the mean molecular weight at the reference temperature.

#### 2.4 Internal Energy Model

The current state of modeling for internal energy effects in Monte Carlo flow field simulations is the phenomenological model of Borgnakke and Larsen.<sup>4</sup> In this model, transfer of energy between internal and translational modes is allowed, but it is necessary to assume that each species has a fixed number of internal degrees of freedom,  $\zeta_i$ . This is equivalent to assuming a constant specific heat,  $C_{pi}$ , for each species which can be related to the number of internal degrees of freedom via

$$\zeta_i = 2 \frac{C_{pi} m_i}{R_0} - 5 . \quad (24)$$

Alternatively,  $\zeta_i$  can be related to the ratio of specific heats for species  $i$ ,  $\gamma_i$ , by the relation

$$\zeta_i = \frac{5 - 3\gamma_i}{\gamma_i - 1} . \quad (25)$$

The interchange of internal and translational energy will be discussed in Section 4, and the selection of initial conditions will be considered in Section 7.

<sup>4</sup>Borgnakke, Claus, and Larsen, Paul S., "Statistical Collision Model for Monte Carlo Simulation of Polyatomic Gas Mixture," Journal of Computational Physics, Vol. 18, 1975, pp. 405-420.

### 3. INTERNAL REPRESENTATION

#### 3.1 State Vector

Each simulated molecule in the direct simulation Monte Carlo method is represented by a state vector which comprises all of the information the code has with regard to that particular molecule. The state vector has:

- Position element(s) defining the location of the molecule in the coordinate system being used. For axisymmetric simulations, this is a radial and an axial element.
- Three velocity elements. A molecular collision is always considered as a three dimensional event, regardless of the overall dimensionality of the problem. For spatially one dimensional problems it is possible to store only two pieces of velocity information and compute the required three velocity components as needed for collision sampling. This is an example of the frequent tradeoff which must be made between storage and computing requirements.
- A value for the internal energy of the molecule. Note that the basic model does not discriminate between internal modes for a particular species. This can be done, if desired, by introducing separate species for the separate modes.
- An indicator determining the molecular species. This indicator in turn implies all of the properties associated with that species (molecular weight, number of internal degrees of freedom, name, etc.).

- An indicator giving the cell in which the molecule currently resides. It is possible to avoid allocating this particular storage element, but it usually results in enough computational simplification to justify its use.

### 3.2 Reduction to a Reasonable Number of Simulated Molecules

It is clearly impossible to run a computer simulation with anywhere near the same number of molecules that exist in the actual flow problem. The adjustment that is made to make the simulation possible is to artificially increase the cross section, and decrease the number density, by a large factor. It is the product of number density and cross section which determines the collision frequency for a given molecule, and it is the collision frequency which must be correctly simulated if the correspondence between the real and simulated flows is to be correct. This is an essential feature of the direct simulation method which has not always been adequately emphasized. It means that the internal scaling factors do not proceed on a strictly dimensional basis. For example, the scaling factor for cross sections is not the square of the scaling factor for lengths.

### 3.3 Internal Scales

Many problems are more reasonably handled if the internal calculations are carried out with scaled or dimensionless values. This avoids possible problems such as numerical overflow which can cause an execution time error. Such errors can be particularly insidious and difficult to locate in a code whose very essence involves the random combination of numbers. Furthermore, examination of scaled values makes the detection

of erroneous values easier while debugging codes since large exponents are usually indicative of an error when the variables are internally scaled. At SSI, at least, the output is produced in physically meaningful dimensional form. Hence, the scaling that is discussed here is irrelevant (or nearly so) to the interpretation of code output; it is strictly a matter of the internal representation.

The obvious choices for length and velocity scales are  $\lambda_\infty$  and  $v_s$  as defined in Section 2, which are used to nondimensionalize the position and velocity elements of the state vector. There is no need to provide further nondimensionalization of mass beyond representing them in atomic mass units, so none is provided. Hence, the scaling factor for energy is just  $v_s^2$ , which is used to nondimensionalize the internal energy element of the state vector.

Number densities are scaled with respect to the far field reference number density,  $n_\infty$ , which leaves only the cross section scaling factor to be determined. This factor follows from the condition of flow similarity, which requires that the probability of a molecule suffering a collision in traveling a given path length be accurately simulated. This dimensionless probability can be expressed as the product of a cross section times a number density times a path length (at least for small enough path lengths), and it is required that this product be the same for dimensional and scaled representations. This implies that the product of the scaling factors for these three quantities be unity and, therefore, the cross section scaling factor is  $1/(n_\infty \lambda_\infty)$ . The internal scaling factors used for the SSI Monte Carlo codes are summarized in Table 1.

Table 1. Scaling Factors Used for the Internal Representation of Quantities in the SSI Direct Simulation Monte Carlo Codes. All Variables are Defined in Section 2.

Property	Scaling Factor
Length	$\lambda_{\infty}$
Velocity	$v_s$
Time	$\lambda_{\infty}/v_s$
Number Density	$n_{\infty}$
Mass	a.m.u.
Energy	$(\text{a.m.u.})v_s^2$
Cross Section	$1/(n_{\infty}\lambda_{\infty})$

### 3.4 Weighting Factors

Weighting factors are a crucial element of a successful Monte Carlo simulation, allowing trace species to be described with reasonable statistics. The weighting factor is the number of "real" molecules that corresponds to each "simulated" molecule. A "simulated" molecule corresponds to one molecule's worth of storage (one state vector) allocated in the computer, and the weighting factor is its statistical weight. So, for example, the total number density in a cell might be represented

$$n_{\text{cell}} = \sum_{i=1}^P \frac{N_i W_i}{V} \quad , \quad (26)$$

where  $N_i$  indicates the number of simulated molecules of species  $i$  in the cell,  $W_i$  is the weighting factor for the species in that cell,  $V$  is the cell volume and  $p$  is the number of species. The product  $N_i W_i$  that appears in Eq. (26) is termed the number of "real" molecules of species  $i$  in the cell. Note that  $n_{\text{cell}}$  as calculated by Eq. (26) is a scaled value; it would have to be multiplied by  $n_{\infty}$ , as shown in Table 1, to become a dimensional evaluation of the number density.

The weighting factors used in the SSI codes are dependent on cell and species. Hence, flowfields where a given species is much more dominant in one portion of the solution region than another can be accurately represented. It is possible, of course, to make weighting factors functions of other variables, such as velocity, for specialized purposes.

A critical error that can occur in Monte Carlo codes is to have the number of simulated molecules exceed the dimensioned limit of the code. On the other hand, it is generally desirable to have as many molecules as is feasible to obtain good statistics. Resolution of these conflicting considerations is complicated by lack of a priori knowledge of what the species number densities will be as a function of space and time. The way the resolution is achieved in the SSI codes is by a dynamic adjustment of the weighting factors, as required. This keeps the number of simulated molecules more or less constant while allowing the number of real molecules to adjust as the solution evolves. The introduction of weighting factors, with the ability to adjust them as the solution demands, is an important feature of a successful Monte Carlo description.

## 4. COLLISION MECHANICS

### 4.1 Relations for Elastic Collisions

The purpose of this section is to present relations appropriate to the simulation of a collision in a Monte Carlo flowfield code. (The question of how molecules are selected for collisions, which is crucial to the proper simulation of collision frequency, will be taken up in Section 6.) Conservation of momentum implies that the center-of-mass velocity of the the collision pair is unchanged by the collision; and conservation of energy then implies that the magnitude of the relative velocity between the collision partners is also unchanged by the collision.<sup>5</sup> Since the collision is treated as a statistical event, all that remains is to select the direction of the post-collision relative velocity vector from the correct distribution. As mentioned in Section 2.2, collisions in the VHS model are treated as hard sphere collisions when they occur (though they do not occur with the same velocity dependence as do hard sphere collisions). Hence, as far as the collision mechanics is concerned, the model is a hard sphere model. For hard sphere molecules, all directions for the post-collision relative velocity vector are equally likely. This is the chief computational simplicity of the VHS model.

Let the two molecules be identified by subscripts 1 and 2, with  $m$  and  $\vec{v}$  denoting their masses and velocities. If  $i$  and  $f$  indicate initial and final states, then the relations for the collision can be summarized via:

---

<sup>5</sup>Vincenti, Walter G., and Kruger, Charles H., Jr., Introduction to Physical Gas Dynamics, John Wiley and Sons, 1965, pp. 348-356.



$$\vec{v}_{cm} = \frac{m_1 \vec{v}_{1i} + m_2 \vec{v}_{2i}}{m_1 + m_2} , \quad (27)$$

$$v_r = |\vec{v}_{1i} - \vec{v}_{2i}| , \quad (28)$$

$$\cos(\theta) = 1 - 2\beta , \quad (29)$$

$$\sin(\theta) = \sqrt{1 - \cos^2(\theta)} , \quad (30)$$

$$\theta = 2\pi\beta , \quad (31)$$

$$\vec{v}_{rf} = v_r [\cos(\theta), \sin(\theta)\cos(\phi), \sin(\theta)\sin(\phi)] , \quad (32)$$

$$\vec{v}_{1f} = \vec{v}_{cm} + \frac{m_2}{m_1 + m_2} \vec{v}_{rf} , \quad (33)$$

and

$$\vec{v}_{2f} = \vec{v}_{cm} - \frac{m_1}{m_1 + m_2} \vec{v}_{rf} , \quad (34)$$

In these relations, and throughout this report,  $\beta$  indicates a random variable which is evenly distributed on the interval zero to one. Each time that  $\beta$  appears a different evaluation of the random variable is implied. Note that the expression for the post-collision relative velocity vector (Eq. (32)) is not coordinate system specific. The indicated vector components can apply to any locally orthogonal coordinate system, since the direction implied is random. The convenient coordinate system to use, of course, is the coordinate system used to define the velocity elements of the state vector. For axisymmetric simulations this will be radial, azimuthal and axial velocity components.

## 4.2 Simulation of Inelastic Collisions

The SSI codes use the Borgnakke and Larsen<sup>4</sup> phenomenological model for transfer of energy between internal and translational modes. In this model, a collision is assumed to be either perfectly elastic or perfectly inelastic, via a user specified probability. A perfectly inelastic collision is achieved by summing the total pre-collision energy (internal energy of both molecules plus the translational energy of their relative motion, Eq. (4)) and then assigning post-collision values from the equilibrium distribution for collisions with that total amount of energy, taking into account the number of internal degrees of freedom in the two molecules. Note that this model has the ability to relax from a nonequilibrium to an equilibrium state via an effective collision number. The ability to exchange internal energy in such a manner comprises a significant increase in capability for Monte Carlo codes beyond the previous models where molecules had no internal energy. It is this capability which enables the codes to realistically predict the macroscopic effects of polyatomic gas flow.

Let  $\zeta_1$  and  $\zeta_2$  be the number of internal degrees of freedom of the two molecules in an inelastic collision, and  $E_s$  be the total collision energy defined by

$$E_s = E_{ci} + E_{1i} + E_{2i} \quad , \quad (35)$$

where  $E_{ci}$  is the initial translational collision energy defined by Eq. (4), and  $E_{1i}$  and  $E_{2i}$  are the pre-collision internal energies of the two molecules. If  $\xi$  is defined by

$$\xi = E_{cf}/E_s \quad , \quad (36)$$

where  $E_{cf}$  is the post-collision translational energy, then  $\xi$  is selected according to the distribution

$$f(\xi) = A \xi^{1-\omega} (1 - \xi)^b \quad (37)$$

where

$$A = \left[ \frac{\langle \zeta \rangle - \omega}{1 - \omega} \right]^{1-\omega} \left[ \frac{\langle \zeta \rangle - \omega}{\langle \zeta \rangle - 1} \right]^{\langle \zeta \rangle - 1}, \quad (38)$$

$$b = \langle \zeta \rangle - 1, \quad (39)$$

and

$$\langle \zeta \rangle = (\zeta_1 + \zeta_2)/2. \quad (40)$$

The sampling of Eq. (37) is done via a technique that is used frequently in Monte Carlo flowfield codes, the acceptance-rejection method. Equation (37) has been normalized so that the maximum value of the function is unity, and the parameter of the distribution,  $\xi$ , varies from zero to one. The sampling is done as follows:

- Choose a random value of  $\xi$ . I.e., set  $\xi$  equal to  $\beta$ , a random variable.
- Evaluate the distribution function for this value of  $\xi$ , and call it  $f_{\text{test}}$ .
- Get a second random variable, and check to see if it is greater or less than  $f_{\text{test}}$ . If it is greater than  $f_{\text{test}}$ , go back to the first step and repeat the process. If it is less than  $f_{\text{test}}$ , then keep the value of  $\xi$  obtained in the first step.

Note that the probability that any original value of  $\xi$  will be kept is proportional to  $f(\xi)$ . This is an extremely general technique and, as such, is very powerful. It is not always efficient, however, and direct sampling of distributions is usually to be preferred if it can be accomplished. In this

case, if one molecule is monatomic and the other is diatomic, i.e., if  $\langle \zeta \rangle = 1$ , then a direct sampling of the above distribution is achieved, via

$$\xi = \beta^{[1/(2-\omega)]}, \quad (\langle \zeta \rangle = 1) \quad (41)$$

Once  $\xi$ , and therefore the post-collision translation energy, is determined, the magnitude of the post-collision relative velocity is defined via

$$v_r = \sqrt{2E_{cf}/\mu_{12}} \quad (42)$$

For inelastic collisions, this relation takes the place of Eq. (28) in the determination of the post-collision velocity elements of the state vectors.

The remainder of the collision energy must be divided up between the internal modes of the two molecules. If one of the molecules is monatomic (i.e., has zero internal degrees of freedom), then all of the internal energy goes to the other by default. Otherwise, if  $x$  is defined by

$$x = E_{1f}/(E_s - E_{cf}) \quad (43)$$

where  $E_{1f}$  is the post-collision internal energy of the first molecule, then  $x$  is just the fraction of the total post-collision internal energy that ends up in the first molecule.  $x$  is distributed with a probability proportional to  $f(x)$ , given by

$$f(x) = B x^c (1-x)^d \quad (44)$$

where

$$B = [(\langle \zeta \rangle - 2)^{(\langle \zeta \rangle - 2)}] / [c^c d^d] \quad (45)$$

$$c = \zeta_1/2 - 1, \quad (46)$$

and

$$d = \zeta_2/2 - 1. \quad (47)$$

Equation (44) can be sampled via the acceptance-rejection method to determine the allocation of the internal energy for the general case. For the special case of both molecules being diatomic, Eq. (44) becomes singular, with the limit being the trivial case that all distributions of internal energy are equally likely, i.e.,

$$x = \beta, \quad (\zeta_1 = \zeta_2 = 2). \quad (48)$$

For the special case of just one of the molecules being diatomic (molecule 2, for instance), then the distribution for  $x$  can be sampled directly via

$$x = \beta^{(2/\zeta_1)}, \quad (\zeta_2 = 2), \quad (49)$$

with the obvious reciprocal relation applying for  $\zeta_1 = 2$ . The SSI codes recognize these special cases so that the sampling can be expedited when possible, while retaining the full generality of Eqs. (37) and (44) when required.

#### 4.3 Collisions for Molecules with Distinct Weighting Factors

There is an obvious problem when considering a collision between two simulated molecules with distinct weighting factors, since they represent a different number of real molecules. If  $W_U$  and  $W_L$  represent the weighting factors for the two molecules, with  $W_U$  being greater than  $W_L$ , then the collision is always counted as  $W_L$  "events". This is accomplished by always assigning post-collision velocity and energy components to the state

vector of the molecule with the smaller weighting factor, but only changing the components of the molecule with the greater weighting factor some of the time. The probability that the molecule with the greater weighting factor will have its components changed is simply  $W_L/W_U$ . Statistically, this means that for a large number of simulated collisions, each such simulated collision will average out to  $W_L$  real collisions for each species, even though their weighting factors differ. It should be noted that this does violate conservation of momentum and energy on an individual collision basis, but these quantities are conserved in the aggregate over a large number of collisions.

#### 4.4 Reactive Collisions

A realistic simulation of chemical reactions is a crucial element of many problems. If a bimolecular reaction of the form



has an Arrhenius rate constant of the form

$$k = A_r T^n \exp(-E_a/R_0 T) \quad , \quad (51)$$

then it is possible to define a reactive cross section as a function of translational collision energy such that the above rate constant is implied for a gas in translational equilibrium. (In Eq. (51),  $T$  is temperature,  $E_a$  is the activation energy,  $n$  is a dimensionless exponent and  $A_r$  is a prefactor.) The product of reactive cross section,  $\sigma^*$ , times relative velocity can be expressed<sup>3</sup>

$$v_r \sigma^* = \frac{(1 + \delta_{ij}) \sqrt{\pi} A_r}{2R_0^n \Gamma(n + 3/2)} \sqrt{1 - \frac{E_a}{E_c}} (E_c - E_a)^n \quad , \quad (52)$$

where  $\delta_{ij}$  is unity for like reactants and zero for unlike reactants. The probability of a collision resulting in a reaction is given by the ratio of the reactive to the gas kinetic cross section at the existing relative velocity between the molecules.

In the SSI Monte Carlo codes, the following procedure is used to determine which, if any, reaction will occur:

- All possible reactions are identified for the pair of molecules which are selected to experience a collision. If there are no such reactions, the procedure is bypassed.
- The probability of each allowed reaction is calculated by computing the reactive to gas kinetic cross section ratio.
- If somehow the reactive cross section(s) total to a greater value than the gas kinetic cross section (which will rarely be the case) then the probabilities are normalized by their sum.
- The collision is taken to be reactive with a probability equal to the sum of the individual reaction probabilities.
- If the collision is reactive, the reaction that occurs is selected in accordance with its probability.
- If no reaction is decided upon, then the collision is either elastic or inelastic according to the user specified probability.

Equation (52) becomes singular for  $n < -3/2$ , and this procedure cannot handle that case. The major limitation of this procedure is that it ignores the effect of internal energy

in determining whether or not a reaction can occur, assuming that the entire activation energy barrier must be overcome through translational energy. If a specified fraction of the molecular internal energy is allowed to contribute to overcoming this barrier, then the restriction on  $n$  is relaxed somewhat (see Ref. 3), but this feature is not presently implemented in the SSI codes.

#### 4.5 Post-Reaction State Definition

The post-reaction state is simply determined by adding the heat of reaction to the total collision energy (translational plus internal) and then computing reactant state vectors for the products based on this total energy and the reactants center-of-mass velocity, as for inelastic collisions. Although this is clearly an oversimplification, it is quite consistent with the phenomenological nature of the model.

The position state vector components for the products are randomly selected from the position state vector components of the reactants, which are not the same (see Section 6). The major additional complication of chemical reactions is that of distinct weighting factors. Since the reaction is  $W_L$  "events" (see Section 4.3), it only destroys the reactant with the greater weighting factor with a probability of  $W_L/W_U$ . If  $W_p$  is a product weighting factor, it is necessary to produce  $W_L/W_p$  simulated molecules of that product. In general this is not an integer quantity, so it is necessary to interpret the ratio statistically so that the expectation value is proper. That is, sometimes the next lower integer is selected and sometimes the next higher one, with a probability that reflects how close each integer value is to the desired fractional quantity. (See the discussion of molecular cloning in Section 5.2.) Of course, the



weighting factors for the two products will in general be different, resulting in a different number of simulated molecules being produced for the two products. Sometimes this process could result in a very large production of simulated molecules for a product with a small weighting factor. In order to prevent overflow of code dimensions it is necessary for the code to sense when this is happening and automatically increase the product weighting factor to prevent it.

#### 4.6 Dissociative Reactions

The situation for dissociative reactions is somewhat complicated by the presence of three rather than two products. With a little manipulation, however, it is possible to use the previous relations for this case as well. Let  $M_1$ ,  $M_2$  and  $M_3$  represent the three product molecules from a dissociative reaction, with a known center-of-mass velocity and total energy. The procedure for defining the post-reaction state is to first define an artificial complex comprised of the  $(M_2, M_3)$  pair. (There is no implication that there actually is any such collision complex.) The complex is assigned a number of internal degrees of freedom equal to  $\zeta_c$ , given by

$$\zeta_c = \zeta_2 + \zeta_3 + 2(2 - \omega) \quad , \quad (53)$$

where the last term represents the contribution of the relative translation between  $M_2$  and  $M_3$ .

The fact that this term is not simply three, as it would seem it should be, merits some explanation. It is due to the fact that these molecules are not random samples from the gas but rather special molecules owing to their being created in a reaction. This point can perhaps best be seen by considering microscopic reversibility, where the inverse reaction is a

three body recombination. For this reverse process, molecules participating in it are not all equally probable, since those with greater relative velocities are more likely to collide. Hence, the term does take on the value three for the special case of  $\omega$  equal to  $1/2$ , which is precisely the case of collision frequency being independent of relative velocity. Examination of Eqs. (37) and (44) demonstrates that translational energy in collisions behaves like another source of internal energy with  $2(2 - \omega)$  degrees of freedom.

With the number of degrees of freedom defined, the separation of  $M_1$  from the  $(M_2, M_3)$  complex is treated as an inelastic collision. The resulting velocity for the complex is then treated as the center-of-mass velocity for  $M_2$  and  $M_3$ , and the internal energy assigned to the complex becomes the total energy for the pair. Using these values,  $M_2$  and  $M_3$  are then separated in another application of the rules for inelastic collisions.

## 5. MOLECULAR TRANSLATIONS

### 5.1 Translation in an Axisymmetric Coordinate System

As discussed in Section 1, an essential element of the direct simulation Monte Carlo method is the periodic advancement of simulated molecules along their trajectories. Formally, this is accomplished by updating the position and velocity elements of the state vector. For a cartesian coordinate system this is a trivial process, but the relations are slightly more complicated for the often used axisymmetric coordinate system. Let  $v_{r0}$ ,  $v_{\phi0}$ , and  $v_{z0}$  represent the initial radial, azimuthal and axial velocity components of a molecule, with  $r_0$  and  $z_0$  representing its initial radial and axial position. Additionally, let  $\phi_0$  represent the initial azimuthal angle for the molecule.

This is included here just for demonstration purposes; it will not generally be known, nor, as will be shown, will it be needed.

The initial position and velocity of the molecule can then be referenced to a standard cartesian coordinate system, yielding

$$\begin{aligned}
 \vec{v}_0 &= \left[ v_{r0} \cos(\phi_0) - v_{\phi 0} \sin(\phi_0) \right] \hat{i} \\
 &+ \left[ v_{r0} \sin(\phi_0) + v_{\phi 0} \cos(\phi_0) \right] \hat{j} \\
 &+ v_{z0} \hat{k} \\
 &= v_{x0} \hat{i} + v_{y0} \hat{j} + v_{z0} \hat{k}
 \end{aligned} \tag{54}$$

and

$$\begin{aligned}
 \vec{r}_0 &= \left[ r_0 \cos(\phi_0) \right] \hat{i} + \left[ r_0 \sin(\phi_0) \right] \hat{j} + z_0 \hat{k} \\
 &= x_0 \hat{i} + y_0 \hat{j} + z_0 \hat{k} .
 \end{aligned} \tag{55}$$

After a time increment  $Dt$ , the position vector of the molecule will be

$$\begin{aligned}
 \vec{r}_1 &= (x_0 + v_{x0} Dt) \hat{i} + (y_0 + v_{y0} Dt) \hat{j} + (z_0 + v_{z0} Dt) \hat{k} \\
 &= x_1 \hat{i} + y_1 \hat{j} + z_1 \hat{k} ,
 \end{aligned} \tag{56}$$

and, in the absence of perturbing forces, the velocity vector will remain unchanged in the cartesian coordinate system. It will change in the axisymmetric coordinate system since the basis vectors are a function of position and the molecule has moved. The new radial position is

$$\begin{aligned}
r_1 &= \sqrt{x_1^2 + y_1^2} \\
&= \sqrt{(r_0 + v_{r0} Dt)^2 + (v_{\phi 0} Dt)^2} ,
\end{aligned} \tag{57}$$

and the new axial position is

$$z_1 = z_0 + v_{z0} Dt . \tag{58}$$

The radial velocity component in the coordinate system appropriate to the new molecular position can be determined by noting

$$\begin{aligned}
v_{r1} &= (\vec{v}_0) \cdot (\vec{r}_1)/r_1 \\
&= \left[ v_{r0}(r_0 + v_{r0}Dt) + v_{\phi 0}(v_{\phi 0}Dt) \right] / r_1 .
\end{aligned} \tag{59}$$

and it can similarly be shown that

$$v_{\phi 1} = v_{\phi 0}(r_0/r_1) \tag{60}$$

and

$$v_{z1} = v_{z0} . \tag{61}$$

Equations (57) - (61) give the updated position and velocity elements of the state vector for a translation in an axisymmetric coordinate system. Note that these relations are indeed independent of  $\phi_0$ . A similar procedure applies for molecular translation in other coordinate systems.

## 5.2 Molecular Cloning

When a simulated molecule is translated from one cell to another, the weighting factor for that species will generally be different in the new cell. Since it is the number of real molecules rather than the number of simulated molecules which

must be preserved when crossing cell boundaries (statistically, at least), it is necessary to correct for the distinct weighting factors (see Section 3.4).

If the weighting factor before translation is  $W_0$ , then the simulated molecule represents that many real molecules. If the weighting factor in the new cell is  $W_1$ , then  $W_0/W_1$  simulated molecules would be required to represent the same number of real molecules in the new cell. If this ratio were a whole integer, then this could be accomplished by introducing that many "clones" of the molecule in the new cell. That is, that many simulated molecules would be placed in the new cell, all with the same state vector.

When the number  $W_0/W_1$  is not an integer (the usual case, of course), then the cloning must be done on a statistical basis. So, for instance, if  $W_0/W_1$  were equal to 2.7, then 30% of the time two clones would be produced and 70% of the time three would be produced. Note that the ratio may be less than unity, and the molecule may not be introduced into the new cell at all. (In which case the molecule is removed from the simulation.)

Cloning is a necessary evil inherent in a system with spatially dependent weighting factors. It enables such a system to maintain the statistically correct flux of mass and momentum across cell boundaries, but it misrepresents the flux of randomized or thermal energy. This can be seen by an extreme case where a very large number of clones is produced when a simulated molecule crosses a cell boundary. The resulting molecules in the new cell have the correct mass and momentum flux, but since they all have precisely the same velocity they have a null relative velocity, and therefore a zero temperature. If the weighting factors are not too different between adjacent cells,

then the errors introduced by this process are acceptably small. However, it does mean that one cannot arbitrarily improve statistics in one portion of the solution region by selectively reducing the weighting factors there. This was a difficulty which was encountered in the early stages of the direct simulation Monte Carlo method while trying to improve statistics along the axis of axisymmetric simulations, since the cell volumes (and therefore the sample sizes) tend to be smallest on the axis.

As was the case for simulated molecules produced via chemical reactions, it is possible for the weighting factors between successive cells to be so different that a prohibitively large number of simulated molecules would be required to produce the same number of real molecules. This is most frequently the case when a new species is being introduced, since before the species gets there the weighting factor is initialized to a very small number. The codes sense when a disproportionate number of simulated molecules are being produced for a given species and cell, and adjust the weighting factor automatically. As the weighting factor is increased, a proportionate fraction of molecules of that species and cell are removed from the simulation in order to keep the number of real molecules properly represented. This process enables the weighting factors to seek their own proper level without a priori knowledge of the solution. (Periodically, the cells are examined to determine if a certain species has been underrepresented in terms of number of simulated molecules. If it is found to be the case, then the weighting factor is decreased, allowing weighting factors to float downwards as well as upwards. It is the danger of weighting factors being too small, causing an overflow of code dimensions, which is most critical, however.)

## 6. COLLISION SAMPLING IN A MULTI-COMPONENT VHS GAS

### 6.1 General Considerations and Approach

The two general considerations in the sampling of collisions are, as usual, accuracy and efficiency of the simulation. As far as accuracy is concerned, it is crucial that the method in which molecules are selected for collisions be proper. It is imperative that the correct collision frequencies be simulated between various species, and, in fact, between the different portions of the velocity phase space for the various species. Furthermore, this frequency of simulated collisions must remain correct without any requirements put on the velocity distribution function; it certainly must not be assumed that there is a Maxwellian velocity distribution.

As far as efficiency is concerned, it is highly desirable to use a method of collision sampling involving a computational effort which is proportional to the number of simulated molecules,  $N$ , in a cell. Methods which are proportional to a power of  $N$  greater than unity can become prohibitively time consuming as the number of molecules is increased - a limit which should be made as accessible as possible for obvious physical reasons.

### 6.2 Collision Sampling for a Single Component Gas

The simplified situation of a simulation involving only one species is considered here. This problem is significant in part due to all the attention it has received and, as will be seen, it serves as an important reference case. When there is just one species, then there is just one gas kinetic cross section (though it is still, of course, a function of collision energy), just one molecular weight and just one weighting factor for each cell. In short, just one of everything that has a

molecular subscript. Hence, in this subsection all such quantities will be presented without subscripts. The most important simplification of having a single species is that there is just one collision class, i.e., only self-collisions of the given species with itself are possible.

#### 6.2.1 Collision Pair Selection

As discussed in Section 1, in the direct simulation Monte Carlo method collisions are sampled on a cell by cell basis until the number of collisions simulated is appropriate to the overall solution time step,  $\Delta t_m$ . The only spatial requirement placed on potential collision partners is that they be within the same cell. In particular, it is not required that they be within a molecular diameter of each other. (Note that if all pairs of molecules were inspected to find those that were sufficiently close to each other, this would involve a computational effort in proportion to the square of the number of molecules in the cell.) The rationale for this is that the cells should be taken small enough such that macroscopic properties can be assumed constant across the cell. When this is the case, then a molecule within the cell can be considered typical of a molecule which might exist anywhere within the cell, and molecular location can be ignored when selecting potential collision pairs.

Spatial consideration aside, the probability of any two molecules experiencing a collision is proportional to  $\sigma c_r$ , the product of their mutual cross section times their relative velocity. This probability is correctly simulated via an application of the acceptance-rejection method if pairs of molecules are selected at random, and then kept or rejected as collision partners with a probability proportional  $\sigma c_r$ . This



is accomplished by keeping a maximum value for  $\sigma c_r$  for each cell (which is updated if a larger value is encountered) and computing the ratio  $r$  defined by

$$r = \frac{\sigma c_r}{(\sigma c_r)_{\max}} \quad . \quad (62)$$

A random variable,  $\beta$ , is then generated, and the pair of molecules is accepted as collision partners if  $r$  is greater than  $\beta$ . This produces the proper relative collision probability without regard to the existing velocity distribution function.

#### 6.2.2 Collision Time Counter for a Single Component Gas

The volumetric collision frequency for a single component gas,  $\nu$  (collisions per unit volume per unit time), is given by

$$\nu = \frac{1}{2} n^2 \overline{\sigma c_r} \quad , \quad (63)$$

where, as in Section 2,  $n$  represents the number density of the species and  $\overline{\sigma c_r}$  is the average product of collision cross section and relative velocity. At first inspection, it would seem from Eq. (63) that a correct simulation of collision frequency would require evaluation of  $\overline{\sigma c_r}$ , which would mean that all pairs of molecules in a cell would have to be considered. Such a procedure involves a computational effort proportional to  $N^2$  and is to be avoided, if possible, in preference to a method which is simply proportional to  $N$ .

The alternative approach, introduced by Bird, is the time counter approach. For each collision a time counter,  $t_c$ , is incremented by an amount that depends on the relative velocity of the collision. Collision sampling continues in a cell until its time counter has been advanced beyond the overall flow simulation time, at which time the code proceeds to the next

cell (which has its own time counter). The time counter increment,  $\Delta t_c$  is given by

$$\Delta t_c = \frac{2}{Vn^2\sigma c_r} , \quad (64)$$

where  $V$  is the cell volume and  $n$  is the species number density given by

$$n = NW/V , \quad (65)$$

with  $W$  being the weighting factor for the species. (Equation (65) is just a special case of Eq. (26).) It should be stressed that Eq. (64) applies for each real collision. As is discussed in Sections 3.4 and 4.3, each simulated collision corresponds to  $W$  real collisions, so when a simulated collision occurs the actual applied increment to  $t_c$  is  $W$  times the value given by Eq. (64).

It is not obvious that Eq. (64) will lead to a proper simulation of the overall collision frequency, so a demonstration will be presented. Let  $f_1(c_r)$  be the normalized distribution function for relative velocity appropriate to a given cell at a given time. (Note that most problems solved by a Monte Carlo technique involve repeated runs, where the total number of collision pairs can be made arbitrarily large. The introduction of a distribution function, and therefore the demonstration of the correctness of Eq. (64) is strictly valid only in the limit of infinitely many runs. Since the essence of the method is a correct statistical representation, it could not be otherwise.) By definition,

$$\int_0^{\infty} f_1(c_r) dc_r = 1 , \quad (66)$$

irrespective of the particular form for  $f_1$ . Let  $f_2(c_r)$  be the normalized distribution function of relative velocity occurring in collisions. Since collisions occur with a probability proportional to  $\sigma c_r$ ,  $f_2$  can be constructed from  $f_1$  via

$$f_2(c_r) = f_1(c_r) \frac{\sigma c_r}{\overline{\sigma c_r}} \quad , \quad (67)$$

where  $\overline{\sigma c_r}$  can now be formally defined via

$$\overline{\sigma c_r} = \int_0^{\infty} f_1(c_r) \sigma c_r dc_r \quad . \quad (68)$$

(Note that in Eq. (68), as in the rest of this demonstration, the functional form of the dependence of cross section on relative velocity need never be specified. The time counter represented by Eq. (64) is therefore not restricted to any particular model for the cross section.)

The average increment of the time counter that is applied over many simulated collisions is therefore given by

$$\overline{\Delta t_c} = \int_0^{\infty} f_2(c_r) \Delta t_c(c_r) dc_r \quad . \quad (69)$$

If Eqs. (64) and (67) are substituted into Eq. (69), the result is

$$\overline{\Delta t_c} = \frac{2}{n^2 V \overline{\sigma c_r}} \quad , \quad (70)$$

where the normalization condition (Eq. (66)) has been utilized. The implication of Eq. (70) is that, on average, the frequency of collisions in the cell is  $V n^2 \overline{\sigma c_r} / 2$ . Since this is simply

the product of cell volume times the proper volumetric collision frequency (Eq. (63)), the validity of the time counter given in Eq. (64) has been demonstrated.

### 6.3 Collision Class Sampling in Gas Mixtures

The above procedure for a single species gas can be extended to a multi-component mixture via consideration of distinct collision classes. In this approach, collision classes are defined by the colliding pair identities. Hence, if there are  $p$  species in the simulation then there are  $p(p+1)/2$  collision classes, which can be identified by the subscripts of the corresponding molecular pair. (The number of classes is not  $p^2$  since the order of molecule specification is not taken to matter in determining a collision class. Hence, the class identified by the subscripts  $i,j$  is not distinct from the class identified by the subscripts,  $j,i$ .)

In collision class sampling, which is the method used by Bird,<sup>1</sup> each collision class is sampled separately, and the collision sampling in a cell is not complete until all classes have been considered. Each collision class has its own stored value of  $(\sigma_{ij}c_r)_{\max}$ , and its own separate time counter,  $t_{cij}$ . By a comparable analysis to that presented above, it can be shown that the appropriate time counter increment in this case is

$$\Delta t_{cij} = \frac{(1 + \delta_{ij})}{n_i n_j V \sigma_{ij} c_r} \quad , \quad (71)$$

where, as in Section 4,  $\delta_{ij}$  is the Kronecker delta which is unity for  $i = j$  and zero otherwise. As in the previous section, the above increment applies for each real collision. A simulated collision corresponds to  $W_L$  real collisions, where  $W_L$  is

the lesser of  $W_i$  and  $W_j$  (see Section 4.3), so when a simulated collision occurs, the applied increment to  $t_{ci}$  is  $W_L$  times the result of Eq. (71).

#### 6.4 Global Collision Sampling in a Gas Mixture

Although the procedure described above is quite reasonable for, say, a two component mixture, it becomes quite complicated as the number of species increases. For 10 species, for instance, the program must loop over 55 distinct collision classes for each cell, and storage must be allocated for 110 quantities in each cell. As the number of species increases, the storage requirement for the collision sampling constants quickly becomes greater than the storage required for the molecular state vectors! The obvious simplification is to search for a technique where collisions are simulated simultaneously for all collision classes, with each class having its proper relative probability of being selected. The overall collision sampling then continues until a single time counter indicates that sufficient collisions have been sampled in the current time step and cell.

##### 6.4.1 Global Collision Time Counter

If molecular pairs are selected for collisions such that the various collision classes automatically appear with the proper relative frequency (see below), then it is not necessary to consider separate time counters for all the various collision classes. One approach that could then be applied is to keep a collision time counter for just one collision class, and increment it when collisions of that class occur. If the various collision classes are being selected according to their correct relative frequency, then simulating the proper frequency for one collision class will ensure, in the long run, that all

collision classes are occurring with the correct frequency. A disadvantage with this approach is the necessity of making an arbitrary choice for the collision class which is to have a time counter. Furthermore, there may be no good choice in a reacting flow where the dominant species may vary strongly from place to place. (Clearly, one would not want to select a class of collision that does not occur in a given cell, since the result would be a never ending sampling of collisions of other classes.)

The preferred approach is to define a global collision time counter,  $t_g$ , which is a weighted average of the time counters of all collision classes; i.e.

$$t_g = \frac{\sum_{i=1}^p \sum_{j=1}^i D_{ij} t_{cij}}{\sum_{i=1}^p \sum_{j=1}^i D_{ij}}, \quad (72)$$

where the  $D_{ij}$  are nonnegative coefficients which can be selected at will. Note that in this formulation every collision will result in some increment of the global time counter (unless  $D_{ij} = 0$  for that class), so the collision sampling frequency is not dependent on any one collision class.

It remains, of course, to specify the  $D_{ij}$ . A very convenient choice is given by

$$D_{ij} = \frac{n_i n_j}{(1 + \delta_{ij})}. \quad (73)$$

Firstly, Eq. (73) is convenient because it tends to make the collision classes with the higher collision frequencies count more, resulting in good statistics for  $t_g$  irrespective of cell

location. (Note that  $D_{ij}$  is cell dependent since the species number densities are cell dependent.) Secondly, Eq. (73) results in a particularly convenient form for  $t_g$ . The normalizing factor in the denominator of Eq. (72) can be summed to give

$$t_g = \frac{2}{n^2} \sum_{i=1}^P \sum_{j=1}^i \frac{n_i n_j}{(1 + \delta_{ij})} t_{cij} \quad (74)$$

Hence, a collision of class  $ij$ , which would produce an increment of  $\Delta t_{cij}$  to its own time counter produces an increment  $\Delta t_g$  to  $t_g$  given by

$$\Delta t_g = \frac{2}{n^2} \left( \frac{n_i n_j}{1 + \delta_{ij}} \right) \Delta t_{cij} \quad (75)$$

where, again,  $n$  is the total number density of all species in the cell. If eq. (71) is substituted into Eq. (75), the result is

$$\Delta t_g = \frac{2}{v n^2 \sigma_{ij} c_r} \quad (76)$$

Equation (76) is extremely significant since it recaptures the precise form of the time counter increment for a single species (Eq. (64)), but indicates that it is completely valid for a multi-component mixture so long as the various collision classes are sampled with the proper relative frequency.

#### 6.4.2 Collision Pair Selection in Multi-Component Mixtures

When considering selection of collision pairs, it is crucial to remember the distinction between real and simulated molecules discussed in Section 3.4. Given two simulated

molecules selected at random from within the cell, the probability of their having a real collision is proportional to  $W_i W_j \sigma_{ij} c_r$ . However, real collisions cannot happen individually; they come  $W_L$  at a time, where  $W_L$  is the lesser of  $W_i$  and  $W_j$ . Hence, when a collision is decided upon in the program,  $W_L$  of them will occur. To compensate for this, potential collision pairs should be accepted for collision according to the size of  $Q$  given by

$$Q = W_U \sigma_{ij} c_r \quad . \quad (77)$$

The relative frequency of real  $ij$  collisions will then be proportional to the product  $QW_L$  (the relative probability of a pair being accepted for collision times the number of real collisions occurring when the pair is accepted), which is the desired relation. Selection of collision pairs with the correct relative frequency then assures that incrementing the global time counter as discussed above will give a statistically correct sampling of all collision classes simultaneously.

#### 6.4.3 Summary of Collision Sampling in Multi-Component Mixtures

The results of this section can be summarized via the following procedure for the sampling of collisions:

- Each cell has a (current) maximum value of  $Q$ ,  $Q_{\max}$ , that has been encountered so far in the collision sampling process. Whenever a larger value is encountered,  $Q_{\max}$  is set equal to that larger value.
- Each cell has a current value of the global time counter,  $t_g$ .
- Pairs are selected at random from all molecules within the cell.
- For each pair,  $Q$  (as defined by Eq. (77)) is computed.



- The ratio of  $Q$  to  $Q_{\max}$  is computed, and a random variable is generated. The pair is accepted for collision if the random variable is less than the ratio. (If the pair is not accepted, then another random pair is selected. The process continues until a pair is accepted.)
- For an accepted pair, the collision mechanics are computed as described in Section 4. This always corresponds to  $W_L$  collisions.
- The global time counter is incremented by  $W_L \Delta t_g$ , where  $\Delta t_g$  is given in Eq. (76).
- The process continues until the global time counter goes beyond the overall flow time. At that point, the collision sampling is commenced in the next cell.
- When all cells have had collisions simulated, then the code proceeds to the translation portion. (See Sections 1 and 5.)

## 7. INITIAL AND BOUNDARY CONDITIONS

### 7.1 General Considerations

The initial and boundary conditions necessary to simulate a problem frequently do not receive their fair share of consideration. It is these conditions which usually distinguish one solution from another, and their correct and efficient specification should be a central concern. Nonetheless, there is clearly room for advancements, particularly in the specification of boundary conditions. Many gas dynamic solutions involve boundary conditions specified at infinity, which are currently simulated by placing boundaries very far from the main flow region. It would result in a substantial computational simplification if boundary conditions applicable closer in to the flow region of interest could be generated for free gas boundaries. Wall boundary conditions also frequently involve a fair degree

of approximation, usually taking the form of accommodation coefficients (though in this case the problem is as much a lack of basic physical understanding of the gas-surface interaction process as it is a lack of a good numerical simulation).

## 7.2 Initial Conditions

Since the direct simulation Monte Carlo method is inherently an unsteady technique, an initial state must be specified in order to advance the solution. (For situations where a steady state result is desired, it is obtained as the long time solution to an unsteady problem. In this case the initial conditions have no effect on the eventual solution, but they may well have an impact on the speed with which that state is achieved.) It will be assumed here that the initial conditions correspond to a uniform flow with the translational and internal modes being in equilibrium. The specification of the initial conditions therefore involves determining the state vector elements consistent with this condition for the desired number of molecules.

### 7.2.1 Number of Simulated Molecules and Weighting Factors

The desired number of simulated molecules of each species in each cell (referred to here as  $M_c$ ) will usually be an input quantity. (Typically, simulations aim for a total number of molecules per cell in the neighborhood of twenty.) Given the initial number density to be simulated for a species,  $n_i$ , (which will have been converted in the code to internal dimensions - see Section 3) the weighting factor for a species in a cell can be derived from an application of Eq. (26) to give

$$W_i = V n_i / M_c \quad , \quad (78)$$

where  $V$  is the cell volume. If a species is not initially present in a cell, then the weighting factor is set to a very small but positive number, typically that which would correspond to an initial mole fraction of one part per million or so. A weighting factor of zero would cause an attempt to divide by zero when molecules of that species move into the cell, but it is generally best to start the weighting factors off small. As the solution proceeds, the weighting factors are automatically adjusted, but the adjustment upward is more direct and immediate than the adjustment downward (see Sections 3.4 and 5.2).

#### 7.2.2 Initial Positions

The initial molecules assigned to a cell should have an equal probability of being placed in any volume element of the cell. The rules for accomplishing this will change with the coordinate system being used, but they are readily derivable from the general principle. As an example, consider an axisymmetric simulation where a cell is bounded by the radial positions  $r_1$  and  $r_2$  ( $r_1 < r_2$ ), and the axial coordinates  $z_1$  and  $z_2$  ( $z_1 < z_2$ ). Since the basic volume element in this coordinate system is  $2\pi r dr dz = \pi d(r^2) dz$ , the volume elements will be sampled with equal probability if  $r^2$  and  $z$  are sampled randomly. Hence, a molecule can be assigned axial and radial positions via

$$r = \sqrt{r_1^2 + \beta(r_2^2 - r_1^2)} \quad (79)$$

and

$$z = z_1 + \beta(z_2 - z_1) \quad (80)$$

(Recall that every time the symbol  $\beta$  occurs it implies a separate random variable. In particular, one should certainly not

use the same random variable to determine radial and axial coordinates. The second application would hardly qualify as "random".)

### 7.2.3 Initial Velocity Components

The thermal velocity components for a molecule in translational equilibrium (neglecting, for the moment, any mean flow contribution) should be selected from the normalized Maxwellian velocity distribution,  $f_0(v)$ , given by

$$f_0 = \frac{\alpha}{\sqrt{\pi}} \exp [-(\alpha v)^2] , \quad (81)$$

where

$$\alpha = \sqrt{\frac{m}{2R_0 T_\infty}} , \quad (82)$$

$m$  is the species molecular weight,  $R_0$  is the universal gas constant and  $T_\infty$  is the temperature. Equation (81) applies for each of the molecular velocity components, and must be sampled three times for each molecule that comprises the initial state of the simulation. A method for directly sampling from this distribution, as presented in Ref. 1, is

$$A_1 = 2\pi\beta , \quad (83)$$

$$A_2 = \sqrt{-\log(\beta)}/\alpha , \quad (84)$$

$$v = A_2 \sin(A_1) . \quad (85)$$

After the thermal velocity components are determined for each molecule, then any mean flow velocity is simply added on. The velocities are then transformed to internal units (see Section 3.3).

#### 7.2.4 Initial Internal Energies

The only remaining element of the state vector to be specified is the internal energy. Internal energies for a gas in equilibrium are distributed according to the normalized distribution function  $f_I$  given by

$$f_I = \frac{\xi^{\zeta/2-1}}{\Gamma(\zeta/2)} \exp(-\xi) \quad , \quad (86)$$

where  $\zeta$  represents the number of internal degrees of freedom for the species in question,  $\Gamma$  is the gamma function and  $\xi$  is a dimensionless internal energy, i.e.

$$\xi = E_I / R_0 T_\infty \quad , \quad (87)$$

where  $E_I$  is the internal energy. In general, sampling of Eq. (86) must be done via the acceptance-rejection method. In the present SSI codes  $\zeta$  is restricted to being greater than or equal to two (or the trivial case of  $\zeta$  equal to zero, which just gives  $E_I$  identically equal to zero). If  $\zeta$  is precisely equal to two, then a direct sampling of the internal energy is possible via

$$\xi = -\log(\beta) \quad . \quad (\zeta = 2) \quad (88)$$

In the general case of  $\zeta > 2$ , it proves convenient to first introduce the transformation  $s = \sqrt{\xi}$ .  $s$  is then distributed in proportion to the distribution  $g(s)$  given by

$$g(s) = 2s^{(\zeta-1)} \exp(-s^2) \quad . \quad (89)$$

Since  $g(s)$  is to be sampled via the acceptance-rejection method, it is first necessary to determine its maximum value,  $g_{\max}$ . Standard calculus serves to show that  $g_{\max}$  occurs at  $s = s^*$ , where

$$s^* = \sqrt{(\zeta - 1)/2} \quad , \quad (90)$$

so

$$\frac{g(s)}{g_{\max}} = \left(\frac{s}{s^*}\right)^{\zeta-1} \exp[s^{*2} - s^2] \quad . \quad (91)$$

The sampling of Eq. (89) proceeds as follows:

- A value of  $s$  is selected randomly from the interval  $s_{\min}$  to  $s_{\max}$ , where

$$s_{\max} = s^* + 5 \quad (92)$$

and

$$s_{\min} = \text{greater of } \{0, s^* - 5\} \quad . \quad (93)$$

(Note that in this interval  $g(s)$  goes from its maximum value to a value on the order of  $10^{-10}$  its maximum value. The transformation from Eq. (86) to Eq. (89) was made mainly to achieve a probability function which dies off extremely rapidly away from its maximum value, so that very little error is associated with considering a finite subinterval for the sampled variable.)

- $g(s)/g_{\max}$  is calculated via Eq. (91).
- A random variable is generated, and the value of  $s$  is kept if the random variable is less than  $g(s)/g_{\max}$ . Otherwise, the procedure is repeated until a value of  $s$  is accepted.
- When a value of  $s$  is selected, then the internal energy is given by  $s^2 R_0 T_{\infty}$ .

As for all the initial conditions, the codes will automatically then express the values in internal dimensions (see Section 3.3).

### 7.3 Wall Boundary Conditions

Boundary conditions in the direct simulation Monte Carlo technique are applied for both wall and free gas boundaries. In a wall boundary condition, whenever a molecule is simulated to strike the wall some action must be taken. Unless the wall is a condensing boundary the molecule will be reflected, and one of several boundary conditions can be selected. The easiest condition is that of a specularly reflecting wall, where the molecule simply is replaced by its mirror image to keep it within the solution region. Another frequently used condition is that of a perfectly accommodating wall. In this condition, a molecule is reemitted from the wall after being selected from a distribution characteristic of the wall temperature and velocity. To date, wall boundary conditions have not been required in the SSI codes, and they will not be discussed further here. They are discussed at some length in Ref. 1, including the intermediate case of partial accommodation.

### 7.4 Free Gas Boundary Conditions

In many cases, the boundary condition is meant to simulate a region of uniform equilibrium flow. Molecules leave the solution region in the normal course of their trajectories, and they simply disappear from the simulation. Molecules are introduced from outside the boundary as selected from distributions appropriate to incoming molecules in the undisturbed flow. It should be stressed that this is not the same as simply sampling a Maxwellian velocity distribution, since it is the molecular flux across the boundary which must be correctly simulated. Hence, molecules with a large component of velocity inward from the boundary are more likely to be selected than they would be in choosing molecules appropriate to a static distribution as was done for the initial conditions described above.

#### 7.4.1 Incoming Number Flux

The first requirement is to determine the number of molecules which should be introduced across the boundary during the solution time step  $\Delta t_m$ . The incoming number flux,  $q$ , (molecules per unit area per unit time) can be expressed<sup>1</sup>

$$q = n_i \left\{ \exp(-w^2)/\sqrt{\pi} + w[1 + \operatorname{erf}(w)] \right\} / 2\alpha, \quad (94)$$

where

$$w = \alpha u_\infty \cos(\theta), \quad (95)$$

and  $\theta$  represents the angle between the inward surface normal and the mean flow, which has a magnitude  $u_\infty$  (i.e.,  $u_\infty \cos(\theta)$  is the inward component of the mean flow velocity),  $n_i$  is the far field number density of the species of interest and  $\alpha$  is given in Eq. (82).

Equation (94) must be applied for each cell on the boundary and for each species that exists in the ambient. The number of simulated molecules to be introduced into the cell,  $N_b$ , is given by

$$N_b = q A_c \Delta t_m / W, \quad (96)$$

where  $A_c$  is the area of the cell along the boundary and  $W$  is the weighting factor for the species and cell in question.

#### 7.4.2 Incoming Molecular Velocity Components

A coordinate system should be set up locally at the boundary such that one direction is in the direction of the inward normal and the other two directions are perpendicular to it. Velocity components are first determined in terms of this local coordinate system, and then transformed, if necessary, to the



main code coordinate system. In the local coordinate system, the velocity components parallel to the surface are determined as discussed above for initial state molecules, but the inward component of velocity must be selected in proportion to the distribution  $h(v)$  given by

$$h(v) = (v + w) [\exp -(\alpha v)^2] , \quad (97)$$

which must be sampled via the acceptance-rejection method. (Only positive  $v$  is allowed, of course, from the definition of the coordinate system.)

#### 7.4.3 Incoming Molecular Position

An initial entry position should be selected for the molecule such that the flux is randomly distributed. Assuming there is no variation of  $\theta$  across  $A_c$  this means that each area element of the exposed cell area should have an equal probability of being selected. Once the initial entry position is selected, then the molecule should be translated a random fraction of  $\Delta t_m$  along its trajectory to determine its actual location. All of the considerations discussed in Section 5 with regard to molecular translations apply to this translation and, in particular, it must be possible to dynamically adjust the weighting factor as required.

#### 7.4.4 Incoming Molecular Internal Energies

The internal energies are selected as described in Section 7.2.4.

## 8. STATISTICAL SAMPLING OF OUTPUT

### 8.1 General Considerations

It is safe to say that the molecular state vectors as they exist in the computer do not comprise the desired output of the procedure. With rare exceptions, it is usually macroscopic quantities such as temperature, density, mean flow velocity, etc., which are of interest - not the microscopic quantities represented by the state vector components of an individual simulated molecule. The generation of the desired output requires that the macroscopic quantities of interest be represented in terms of statistical sums of the available microscopic quantities; and it is the main purpose of this section to present these correspondences. All sums are kept in terms of "real" molecules and events, i.e., the current weighting factors are included in the sums. This is essential since the weighting factor determines the statistical importance of a given molecule. Since the weighting factors are dynamically and unpredictably adjusted as the solution progresses, it would not be possible to go back and add in the effect of weighting factors a posteriori.

In general, it must be decided ahead of time exactly what output is desired from the code, and therefore what statistical sums should be kept to generate it. There is a vast amount of potential information in the simulation, and it is not reasonable to store all possibly interesting quantities in all runs. On the other hand, it is wasteful to completely rerun a case just because the user decides there was an additional quantity he was interested in. The selection of output for a given run, therefore, unavoidably requires user judgement. Once the user has decided upon the required output, the determination of which

statistical sums should be kept can be done automatically by the code. Care is taken to make sure that a statistical sum is not duplicated internally if it is required by more than one requested output quantity.

Some initial words of caution are required. By its nature, the direct simulation Monte Carlo method works with far fewer molecules than nature does, and it therefore exhibits considerably greater statistical variation in its macroscopic predictions. To reduce these variations, the codes are run repeatedly for the same case, increasing the statistical base from which the macroscopic output is derived. If care is taken to use efficient techniques, such as described in this report, then useful results can usually be obtained with a modest computational effort. This statement must be tempered, however, by a realization of the convergence rate for Monte Carlo sampling. Basically, the statistical error in the output converges as one over the square root of the sample size (or run time). Hence, if a solution looks good, but the user decides he would like one more significant digit (i.e., he would like the statistical error to be reduced to 0.1 times its current value) it would require that the run time be increased by a factor of 100! It can be seen that the desire for more accuracy can very quickly turn the most efficient code into a money gobbling nightmare. When using a Monte Carlo technique, one must accept some statistical scatter in the output.

## 8.2 Sampling of Instantaneous Output Quantities

Instantaneous output quantities are those which are, in principle, derivable from an instantaneous "snapshot" of the solution. These quantities, such as density, temperature and velocity, can be determined by examining the molecular state

vectors at a particular time in the simulation. The code pauses in the simulation and uses the molecular state vector elements to add values to statistical sums appropriate to the various cells and the particular time that it passed. It then proceeds with the simulation until the next sampling time. As the code goes through its successive runs, it stops at the same points in the simulation every time and adds to the statistical base for the sums. The items listed below, with their statistical definitions, are selectable as output requests in the SSI codes. Summations are made over all applicable simulated molecules, which includes  $N_{\text{run}}$  separate runs.

Total Number Density

$$n = \frac{1}{VN_{\text{run}}} \sum_i w_i \quad (98)$$

Mean Molecular Weight

$$m = \frac{\sum_i w_i m_i}{\sum_i w_i} \quad (99)$$

j'th Velocity Component

$$v_j = \frac{\sum_i w_i m_i v_{ji}}{\sum_i w_i m_i} \quad (100)$$

# Overall Translational Temperature

$$T = \frac{1}{3R_0 S_1} \left( S_2 - \frac{S_3^2 + S_4^2 + S_5^2}{S_6} \right) \quad (101)$$

where

$$S_1 = \sum_i W_i \quad (102)$$

$$S_2 = \sum_i W_i m_i (v_{1i}^2 + v_{2i}^2 + v_{3i}^2) \quad (103)$$

$$S_3 = \sum_i W_i m_i v_{1i} \quad (104)$$

$$S_4 = \sum_i W_i m_i v_{2i} \quad (105)$$

$$S_5 = \sum_i W_i m_i v_{3i} \quad (106)$$

$$S_6 = \sum_i W_i m_i \quad (107)$$

# Translational Temperature in j'th Direction

$$T_j = \frac{1}{R_0 S_1} \left( S_7 - S_8^2 / S_6 \right) \quad (108)$$

where

$$S_7 = \sum_i w_i m_i v_{ji}^2 \quad (109)$$

$$S_8 = \sum_i w_i m_i v_{ji} \quad (110)$$

Internal Mode Temperature

$$T_I = \frac{2 \sum_i w_i E_{Ii}}{R_0 \sum_i w_i \zeta_i} \quad (111)$$

with the exception of Eq. (99), all of the above quantities can also be defined and calculated for any specified species. The sums are the same except that only molecules of that species are considered. Before printing output quantities, they are always transformed to standard dimensions from the internal scales.

### 8.3 Sampling of Time Averaged Quantities

Some additional quantities of interest are not sampled at a separate sampling time as described above, but rather as the simulation evolves. Examples of such quantities are collision rates, reaction rates, mean velocities between molecules, etc. In general, these quantities depend on the relative state of more than one type of molecule, and they are by their nature expressed as average values over a finite time interval. The formulas for calculating these quantities are little more than

event counters, and will not be included here. The following quantities are currently available as output:

- Mean Relative Velocity Between any Two Species
- R.M.S. Deviation of Mean Relative Velocity Between any Two Species
- Mean Product of Cross Section Times Relative Velocity Between any Two Species
- Collision Rate Between any Two Species
- Reaction Rate for any Chemical Reaction.

The sampling for all of these quantities occurs in the collision simulation routines. As pairs are considered as possible collision partners, statistics are kept, if necessary, to generate the first three quantities. Statistics on collisions and reactions are kept as they occur.

## 9. APPLICATION TO THE FREEJET EXPANSION WITHIN A MASS SPECTROMETER

### 9.1 Motivation for Studying Major Species Freejet

The freejet expansion of the major (neutral) species through a sonic orifice into a near vacuum is a classic problem representing the zeroth order solution to the problem at hand. The numerical dominance of the major species assures that their distribution in phase space (i.e., their density and velocity distributions) will be negligibly affected by the minor species of interest (e.g., ion clusters,  $H_2O$ , etc.). Hence, for a given atmospheric pressure and orifice geometry the freejet expansion of the major species can be calculated once and for all. The physical processes of interest (ion acceleration due to electric fields, agglomeration, fragmentation, etc.) can then be handled by considering the minor species to be traveling within a known

phase space distribution of major species. Considerable conceptual and computational simplifications result from the recognition that the freejet expansion is uncoupled from the ionic motion.

## 9.2 Physical Description of the Freejet Expansion

The major features of a freejet created by expanding air through a sonic orifice into a near vacuum are illustrated in Figure 1. For the cases of interest (20-40 km altitude, orifice diameter = 0.04 cm) the orifice is always considerably larger than an ambient mean free path, so the initial portion of the expansion is best described in terms of continuum fluid mechanics. The orifice forms a sonic throat in which the flow is accelerated to a Mach number of unity. If the orifice has a finite thickness ("t" in Figure 1), then a boundary layer forms on the edge of the orifice, restricting the flow somewhat from that which would be predicted via one-dimensional inviscid theory. The mass flow through the orifice can be represented by<sup>6</sup>

$$\dot{m} = C_D (\pi r_o^2) \sqrt{\gamma P_o \rho_o} \left[ \frac{2}{(\gamma + 1)} \right]^{\{(\gamma + 1)/[2(\gamma - 1)]\}} \quad (112)$$

where  $r_o$  is the orifice radius,  $\gamma$  is the ratio of specific heats in the gas and  $P_o$  and  $\rho_o$  are the stagnation pressure and density, respectively. The discharge coefficient,  $C_D$ , is a corrective factor to bridge the gap between the ideal and real worlds.  $C_D$  is less than unity due to the presence of the orifice boundary layer (viscosity influence) and two dimensional flow effects.

---

<sup>6</sup>Shapiro, A.H., The Dynamics and Thermodynamics of Compressible Fluid Flow, the Ronald Press Co., New York, 1953, pp. 73-105.



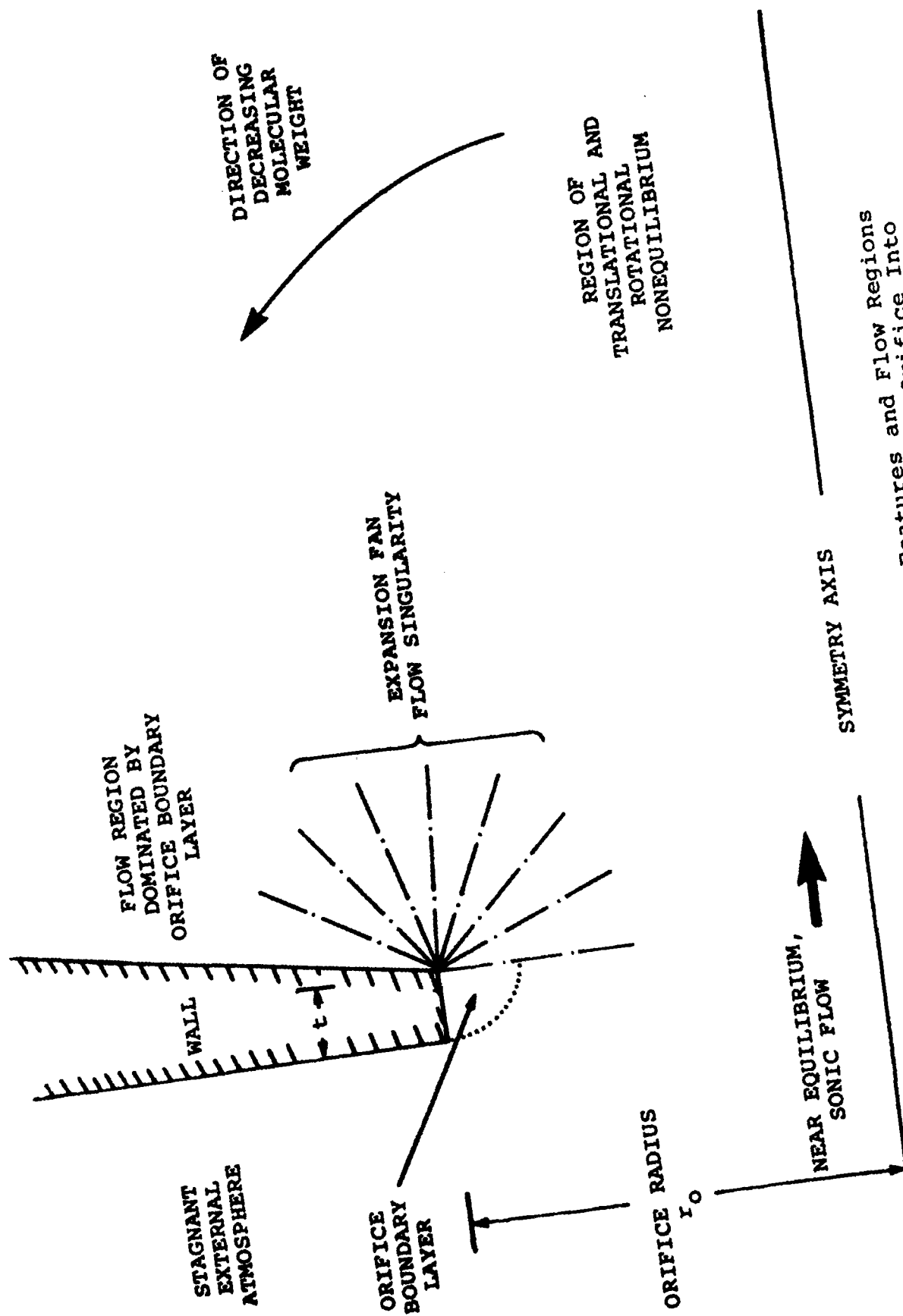


Figure 1. Schematic Showing the Major Features and Flow Regions Involved in The Expansion of a Gas Through a Sonic Orifice Into a Near Vacuum.

As the gas passes through the orifice, an expansion fan is formed on the inner edge of the orifice and spreads out into the flowfield. The expansion fan is initially describable in terms of Prandtl-Meyer theory, but is altered from that form as it proceeds away from the orifice by axisymmetric (as opposed to planar) flow effects.

The initial portion of the supersonic expansion is well suited for calculation via the method of characteristics (MOC),<sup>6</sup> although the interaction of the boundary layer with the expansion fan is difficult to treat analytically. As the flow proceeds away from the orifice the rotational and randomized translational energy is transferred to directed kinetic energy of the flow. The flow expansion, and consequent reduction in collision frequency, causes the gas to depart from thermal equilibrium. A residual rotational energy remains in the gas after collisions cease, and this is often characterized by a rotational temperature. (The populated rotational states do not, in general, adhere to a Boltzmann distribution;<sup>7</sup> but this is of no great consequence to the present investigation.) Furthermore, the expansion is characterized by distinct parallel and perpendicular temperatures representing residual randomized kinetic energy in directions parallel to and perpendicular to the mean flow direction.

The portion of the jet at large angles from the symmetry axis is dominated by the slower, more easily turned, gas from the orifice boundary layer. Also, the lighter molecular weight

---

<sup>7</sup>Sharafudinov, R.G. and Skovorodko, P.A., "Rotational Level Population Kinetics in Nitrogen Freejets," Proceedings of the 12th International Symposium on Rarefied Gas Dynamics, AIAA Press, 1980.

species become more concentrated at large angles from the symmetry axis leaving the central portion of the jet more concentrated in species with heavier molecular weights.<sup>8</sup>

### 9.3 Potential Computational Approaches

For the most part the departure of the freejet from local thermodynamic equilibrium marks the end of the region of validity for continuum techniques such as the method of characteristics. (An exception to this is a recent paper by Labowski, Ryali, and Fenn using the so-called nonequilibrium method of characteristics on a rotationally relaxing freejet.<sup>9</sup> However, the method does not apply when the translational modes go out of equilibrium. Since the region between rotational and translational nonequilibrium is usually small, the method is inappropriate in the present study.)

The only presently available computational technique which is capable of describing the critical molecular processes occurring in the latter portions of the expansion is the direct simulation Monte Carlo method. There is no choice to be made for the calculational technique to be used in the nonequilibrium portion of the expansion; the only question is whether the Monte Carlo method should be used for the entire solution region, or whether it should be wedded to a MOC calculation of the equilibrium portion. The answer to this question depends largely on

---

<sup>8</sup>Bird, G.A., "Breakdown of Continuum Flow in Freejets and Rocket Plumes," Proceedings of the 12th International Symposium on Rarefied Gas Dynamics, AIAA Press, 1980.

<sup>9</sup>Labowski, M. Ryali, S., and Fenn, J.B., "Flowfield Calculations in Nonequilibrium Freejets by the Method of Characteristics," Proceedings of the 12th International Symposium on Rarefied Gas Dynamics, AIAA Press, 1980.

how large the equilibrium region is expected to be. (It should be stressed that the Monte Carlo flowfield is valid for equilibrium continuum flow -- but it is less efficient computationally.)

The breakdown of translational and rotational equilibrium has been considered in some detail by Bird,<sup>8,10</sup> and it has been observed to correlate well with the parameter  $P$  given by

$$P = \frac{1}{\nu} \frac{D(\ln \rho)}{Dt} , \quad (113)$$

where  $\rho$  is the fluid density,  $\nu$  is the collision frequency and  $D/Dt$  represents the substantial derivative with respect to time. The breakdown of equilibrium has been observed to correlate quite well with a  $P$  value of approximately 0.05.

Figure 2 shows contours of constant  $P/Kn$  as calculated in Ref. 8 for the expansion of a diatomic gas from an orifice into a vacuum. In this figure the Knudsen number,  $Kn$ , is defined as the ratio of the mean free path at the orifice to the orifice radius. The calculation was performed via the method of characteristics, so the orifice Mach number was taken to be 1.1 to allow the calculational grid to step away from the orifice.

For the parameter range of interest (altitudes of 20-40 km, orifice radius = 0.02 cm) Figure 2 can be used to estimate the position at which the onset of nonequilibrium occurs, and, hence, the maximum range of validity for a MOC calculation before it must be joined to a Monte Carlo calculation. The conclusion is that a MOC calculation cannot be used beyond two orifice radii from the orifice at 20 km and essentially cannot

<sup>10</sup> Bird, G.A., "Breakdown of Translational and Rotational Equilibrium in Gaseous Expansions," AIAA Journal, Vol. 8, No. 11, November 1970, pp. 1997-2003.

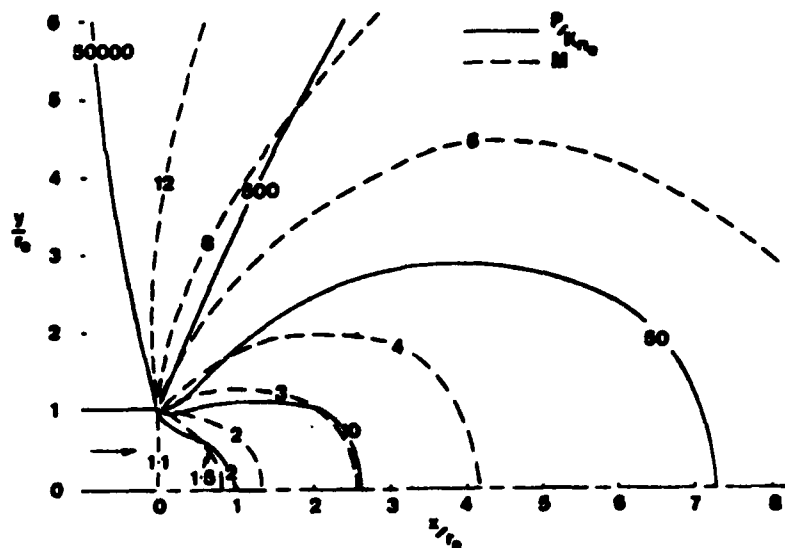


Figure 2. Contours of Mach Number and Continuum Breakdown Criterion in the Freejet Expansion of a Diatomic Gas. (From Reference 8.)

be used at all at 40 km altitude. This very limited range of validity for a MOC calculation strongly suggests that the preferred calculational approach is simply to use a Monte Carlo method for the entire flowfield.

#### 9.4 Cell Mesh Selection

The selection of grid geometries for fluid mechanic calculations can generally be regarded as more of an art than a science. Considerations in the selection of a grid are:

- The grid should be as simple as possible, since the program must repeatedly decide what cell molecules are in as they move. If this required the solution of a complex equation, the entire program would run significantly slower than if the cell can be determined easily.

- The grid should concentrate cells where gradients are the largest, so that the least number of total cells (and molecules) are needed to obtain an accurate solution.
- The grid should provide output where it is required, with the resolution that is desired for the answer of interest.

The cell structure which was introduced in the first quarterly technical report was based mainly on the second consideration listed above. It concentrated cells in the vicinity of the Prandtl-Meyer discontinuity, where the flow gradients are largest. It suffers disadvantages, however, in that spurious small cells occur on the axis and cell determination for a molecule is somewhat difficult. As a first attempt, therefore, a simpler cell structure was devised. The cell structure is illustrated schematically in Figure 3, and is characterized by the following relations:

- The orifice radius is divided up evenly into a specified number of grid spacings. This number can be varied to achieve convergence.
- Above the orifice, at the first axial location, there are some additional cells of the same size to help describe the expansion that occurs around the orifice edge. The number of cells above the orifice can also be varied to achieve convergence along the flow centerline (the region of importance for the present investigation).
- The cells are constructed between a series of planes which are perpendicular to the jet axis. The spacing between successive planes increases as they proceed further from the orifice, since the flow gradients will decrease in this direction. The rule for the increase of the spacing between the planes is given by the equation:

$$\frac{Dz_j}{r_o + z_j} = A = \text{constant} \quad , \quad (114)$$

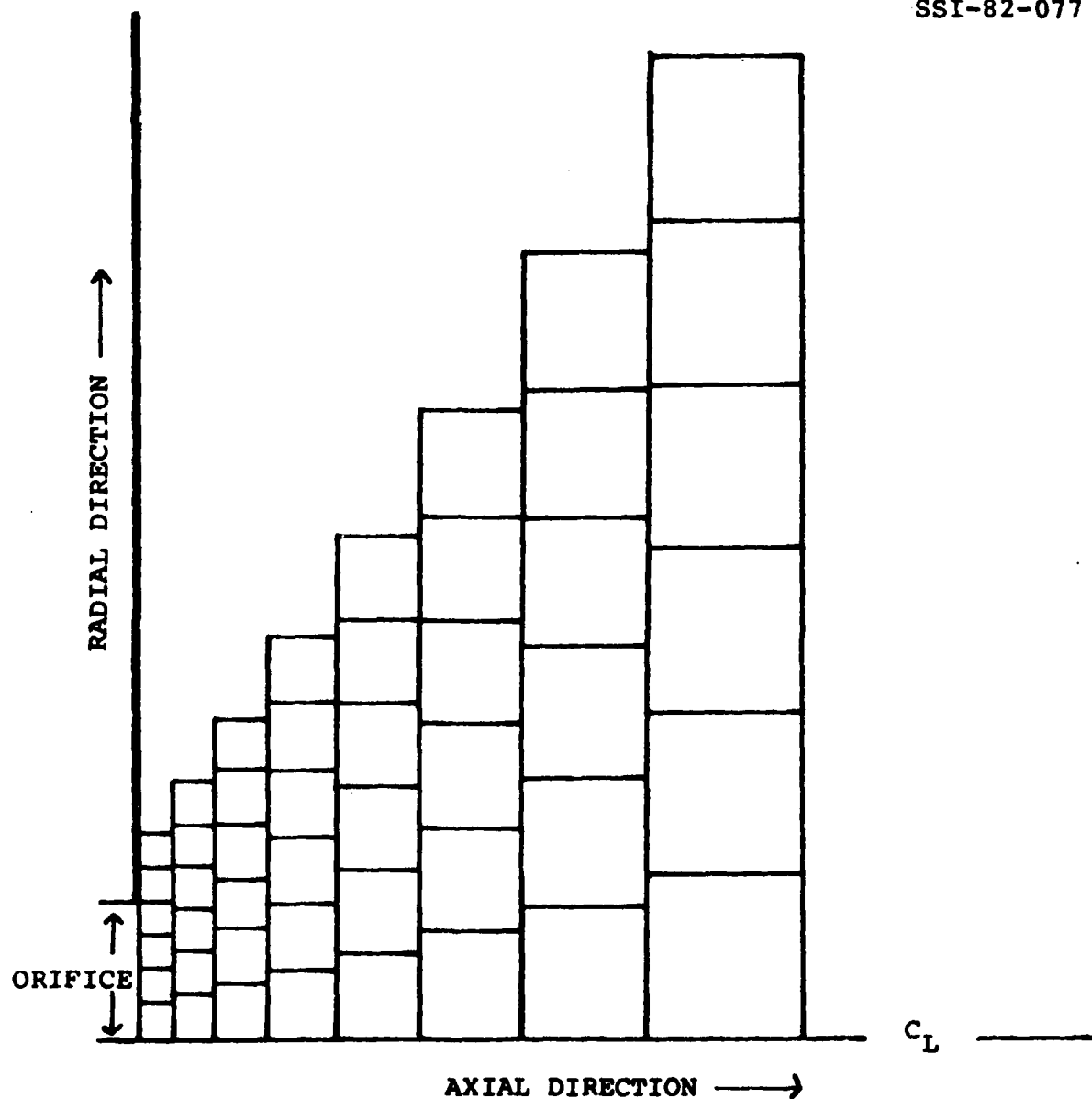


Figure 3. A Drawing of a Cell Mesh of the Type Devised for the Initial Freejet Calculations. The pictured mesh corresponds to the coarse mesh used for the results presented in Figure 4, except that it has been truncated after eight axial cells as opposed to the ten used in Figure 4.

where  $Z_j$  is the location of the  $j$ 'th plane and  $DZ_j$  is the spacing between it and the previous plane (i.e.,  $DZ_j = Z_j - Z_{j-1}$ ), and  $r_o$  is the orifice radius. This relation can be solved to give the location of  $Z_j$  directly as:

$$Z_j = r_o \left\{ \left[ 1/(1-A) \right]^j - 1 \right\} . \quad (115)$$

This relation is easily inverted to find the axial cell location of a particular molecule.

- The cells are selected to have a radial increment equal to the axial increment, and the number of cells per axial location is kept constant. Hence, as the cells grow larger in the axial direction, they automatically keep pace in the radial direction.

## 9.5 Sample Computational Results

Initial calculations were performed for atmospheric conditions appropriate to an altitude to 30 km (ambient number density of  $3.83 \times 10^{17}$  molecules/cm<sup>3</sup>, ambient temperature of 227 K) for a mixture of 79% nitrogen and 21% oxygen. The flow was expanded isentropically to a Mach number of unity at the orifice, and the flow profile was assumed uniform across the orifice. As was discussed previously, this is recognized to represent an idealization; but it seemed like a reasonable place to start the calculations.

The first question that was addressed was to determine what type of grid was required to achieve convergence of the solution. Figure 4 shows plots of axial number density obtained from two separate grid spacings, for otherwise identical runs. The coarser grid divided the orifice radius into four separate cells (which means, of course, that the diameter was divided into eight cells) and had two additional cells above the orifice. The finer grid had twice as many cells within and above the



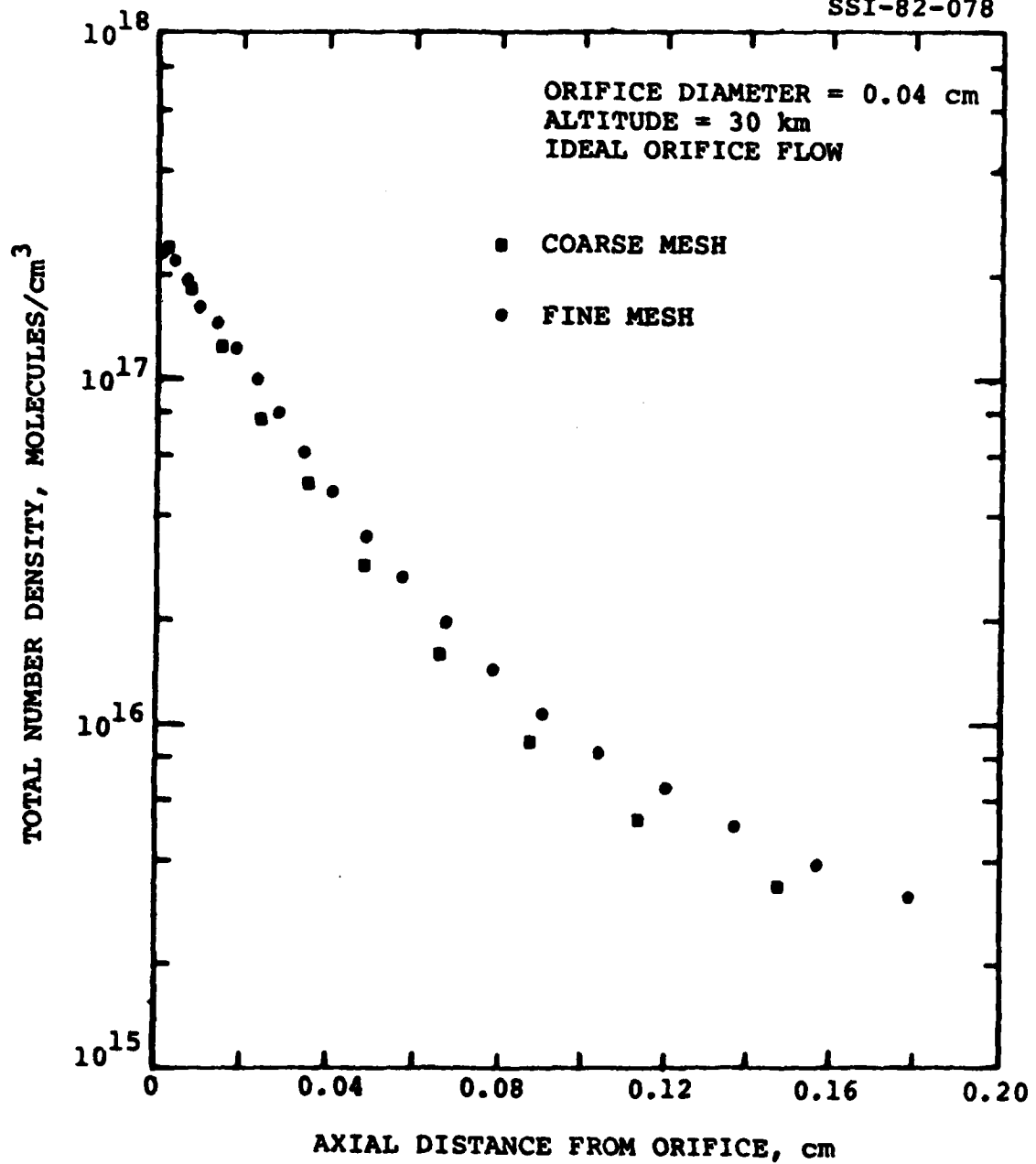


Figure 4. Total Axial Number Density as Calculated for a Coarse and a Fine Cell Mesh. The startline condition for these calculations corresponds to uniform flow across the orifice at a Mach number of unity.

orifice radius. The calculations were carried out for approximately 3.5 orifice diameters downstream (0.15 cm), by which distance the flow was substantially supersonic. This is important since it means that the neglect of molecules traveling upstream into the solution region is quite well justified.

#### 9.6 Discussion of Freejet Calculations

The first conclusion to draw from these preliminary calculations is that the program is working, and the results look reasonable. It can be seen, however, that the coarse grid spacing is not adequate to achieve a convergence of the solution, and, on the basis of these results, it cannot be said whether or not the fine grid spacing is converged. Further calculations will clarify this issue and others regarding mesh convergence. It is also desirable to know how many cells are required above the orifice to achieve accurate axial profiles.

If the required number of cells to achieve mesh convergence for the cell structure outlined in this section is too large, then it may well be necessary to adopt another structure such as the one outlined previously. It is expected that the ideal orifice considered here represents a worst case, since when an actual flow profile is introduced across the orifice, the orifice boundary layer will lessen the importance of the Prandtl-Meyer discontinuity, and therefore the importance of small cells in that region.

Rotational relaxation was calculated for these test cases, and a significantly higher rotational than translational temperature (106 K versus 25 K) was predicted. These numbers have no quantitative significance, since no attempt was made to input a proper rotational relaxation collision number. However, it is noteworthy that the code is capable of predicting this physically real behavior.

## 9.7 Real Orifice Flow Effects

In principle, it would be possible to compute the flow from the undisturbed atmosphere into the mass spectrometer in a single solution. In such a solution, the boundary conditions applied would correspond to:

- 1) An undisturbed atmosphere bounding the appropriate portion of the solution region.
- 2) A wall interaction representing the molecular collisions with the mass spectrometer casing as well as the sides of the orifice.
- 3) Possible downstream conditions if the solution is carried to the point where interaction with the background gas within the mass spectrometer is important.

Although wall boundary conditions do have a degree of approximation that reflects our incomplete understanding of the gas-surface interaction process, the above boundary conditions are relatively well characterized. However, the above procedure does involve a substantial amount of computational effort aimed at the flow outside of the mass spectrometer, since that flow is usually characterized by a relatively small mean free path. Since the primary interest of the present study is to describe the flow within the mass spectrometer, it is natural to try to reduce the size of the solution region while retaining the essential portion of the flow. The obvious way to do this is to approximate the flow at the orifice, and merely compute the flow within the instrument.

There are several reasons to believe that such a procedure would be fruitful. If the orifice were a smooth walled converging-diverging nozzle, then the flow would expand to a Mach number of unity at the orifice plane, and it would be known exactly (except for boundary layer and two dimensional effects) irrespective of

the flow downstream of the orifice. Although the actual orifice has a sharp edge, intuition implies that the downstream flow can have at best a small effect on the orifice flow, so it would seem plausible to specify the orifice flow a priori. Furthermore, the present study is concerned mainly with the flow along the centerline of the resulting jet, where boundary layer and two dimensional effects should be minimized.

Although it would seem to be a classic problem, the expansion from a uniform state through a sharp edged orifice into a vacuum has apparently not been the object of intense study. Liepmann<sup>11</sup> considered the problem in some detail, and indicated that the flow in the plane of the orifice is subsonic along the centerline, going supersonic and then back to sonic as the edge of the orifice is approached. Little else was said in this or any other available reference about the actual flow in the orifice plane. Measurements were presented, but they were limited to the discharge coefficient (the ratio of ideal to actual mass flow), which was subsequently measured by Smetana, Sherrill and Schort<sup>12</sup> to greater accuracy. The results of the latter study are presented in Figure 5, which has been replotted to obtain a more convenient form. (As presented in Ref. 12 both axes involved the unknown mass flow, so an iteration was required to determine the discharge coefficient. This problem is removed when the Reynold's number is defined in terms of available reference quantities rather than the unknown mass flow. The two Reynold's numbers differ only by a factor of the discharge coefficient.)

---

<sup>11</sup>Liepmann, H.W., "Gaskinetics and Gasdynamics of Orifice Flow," Journal of Fluid Mechanics, Vol. 10, No. 5, 1961, pp. 65-79.

<sup>12</sup>Smetana, F.O., Sherrill, W.A., and Schort, D.R., "Measurements of the Discharge Characteristics of Sharp-edged and Round-edged Orifices in the Transition Regime," Proceedings of the 5'th Rarefied Gas Dynamics Symposium, Vol. 2, Academic Press, 1967.

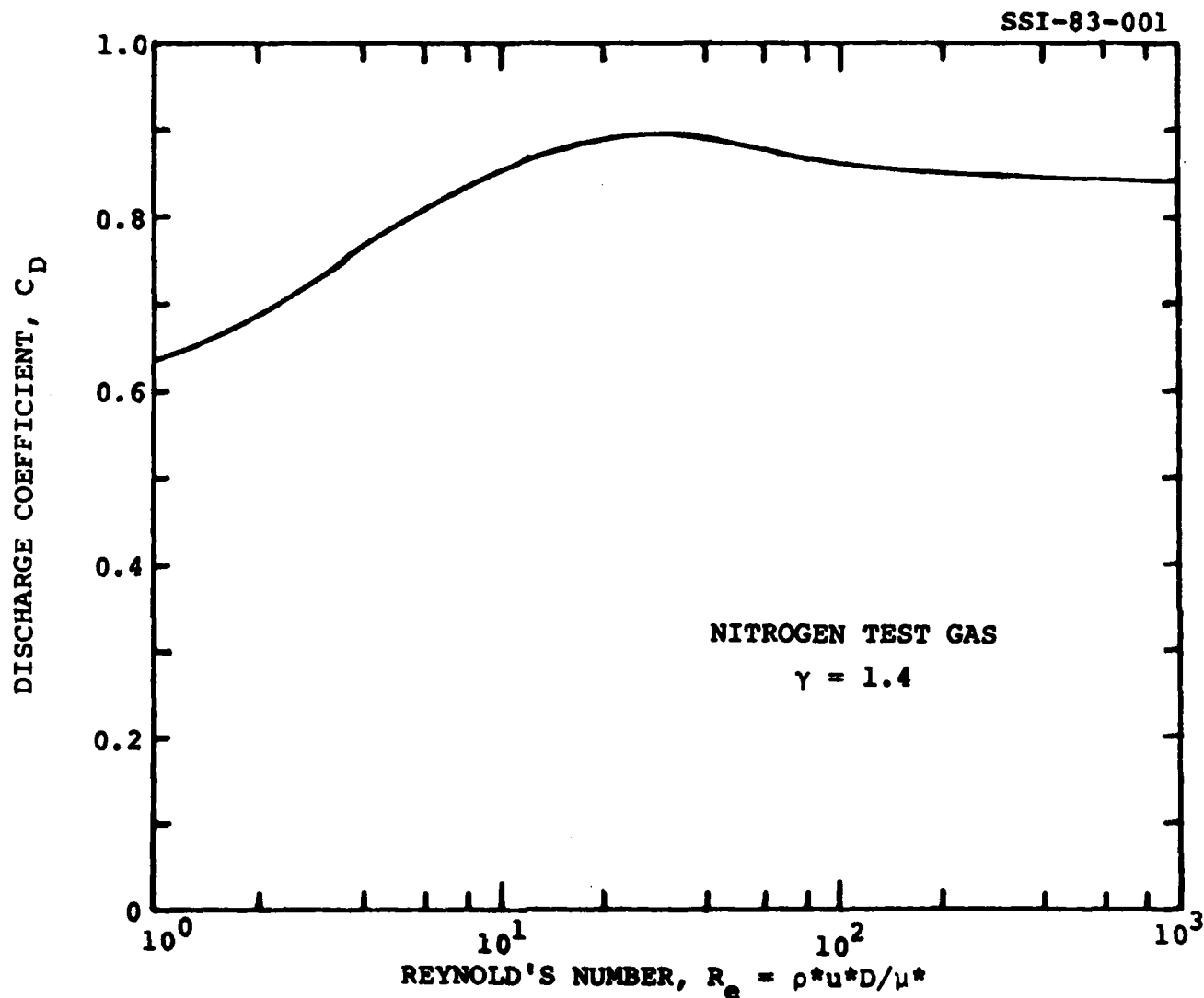


Figure 5. The Discharge Coefficient for a Sharp Edged Orifice as Measured by Smetana, Sherrill and Schort.(3) It is plotted here as a function of Reynold's Number based on sonic conditions and the orifice diameter.

Use of the discharge coefficient presented in Figure 5 accounts for the major effect of a sharp edged orifice as opposed to a smooth nozzle, and it is apparently the only available effect for which measurements exist. The initial approach will be to adjust the orifice mass flow to reflect the results of Figure 5, but the mean flow velocity will still be assumed to start at sonic conditions. (Individual molecules, of course, will have a distribution of velocities. See Section 7 for a complete description of the handling of boundary conditions.) Any error incurred via this procedure should have little effect on the centerline solution of interest.

#### 9.8 Handling of Minor Species

As discussed in Section 6, a procedure has been devised at SSI to handle sampling of collisions simultaneously between an arbitrary number of species. For the mass spectrometer case, however, it may be advantageous to recast this procedure in terms of major and minor species. The solution for the major species can be carried out once and for all for a given altitude and instrument design. Then, since the minor species are too numerically insignificant to affect the major species flow, it is possible to consider several possible atmospheric concentrations of various minor species in order to obtain a best fit with the data. In order for this procedure to work, of course, there has to be a method to go back and calculate minor species distributions given the major species solution. It is the purpose of this section to present that method.

In such a minor species solution, it is only necessary to define a density, velocity and temperature in each cell for each of the major species. (Actually a different effective temperature would be defined for each direction.) Then, for purposes

of sampling collisions between major and minor species, major species molecules can be generated from the proper distribution as needed. These molecules need not be permanently stored, nor is it necessary to advance them along their trajectories.

The major computational advantage, however, is the removal of a necessity for calculating collisions of major species with themselves. Since collision sampling is the most time consuming element of a Monte Carlo simulation, and the collisions between major species are the most prevalent, there is room for a substantial increase in computational speed. Within the framework described in this report, this can be accomplished by defining separate global time counters for major-minor and minor-minor collisions. Each global time counter is defined as a weighted average of the time counters for each collision class that falls within its domain. The weighting factors are selected to achieve tractable forms for the two time counters.

#### 9.8.1 Time Counter for Collisions Between Two Minor Species

Ordinarily, collisions between two minor species would be considered unimportant in comparison to collisions between major and minor species. However, for the present study there are processes such as agglomeration which may not be negligible (due to very large cross sections) even though they involve two minor species. The handling of minor species self-collisions can be achieved exactly as described in Section 6, with the adjustment that total number density is taken to refer to total minor species number density. The time counter increment is then just as given in Eq. (76).

### 9.8.2 Time Counter for Collisions Between Major and Minor Species

A separate global time counter is easily defined for major-minor collisions. If  $P$  denotes the number of major species and  $p$  denotes the number of minor species, then the major-minor collision time counter,  $t_g$ , can be defined via

$$t_g = \frac{\sum_{i=1}^P \sum_{j=1}^p D_{ij} t_{cij}}{\sum_{i=1}^P \sum_{j=1}^p D_{ij}} \quad , \quad (116)$$

which is the obvious extension of Eq. (72). The convenient choice for  $D_{ij}$  proves to be

$$D_{ij} = n_i n_j \quad . \quad (117)$$

(In the above relations, an  $i$  subscript is now taken to refer to a major species, and a  $j$  subscript is taken to refer to a minor species. In Section 6 the subscripts make no such distinction.) Substituting Eq. (117) into Eq. (116), and carrying out the summation in the denominator yields an expression for the major-minor global time counter in terms of the time counters for the individual collision classes. The appropriate increment in the global time counter to make when simulating a collision is

$$\Delta t_g = \frac{1}{V n_I n_J \sigma_{ij} c_r} \quad , \quad (117)$$

where  $n_I$  and  $n_J$  refer to the total number densities of all major and minor species, respectively,  $V$  is the cell volume, and  $\sigma_{ij}$  is the mutual cross section for the species colliding at a



relative velocity  $c_r$ . The time counter increment represented by Eq. (118) is much larger than the increment would be for the same collision (Eq. (76)) if minor species were not being handled separately. This is the quantitative realization of the general principle that collision sampling goes a lot more quickly if major-major collisions need not be considered.

## REFERENCES

1. Bird, G.A., Molecular Gas Dynamics, Clarendon Press, Oxford, 1976.
2. Chapman, Sydney, and Cowling, T.G., The Mathematical Theory of Non-Uniform Gases, 3rd ed., Cambridge University Press, Cambridge, 1970, pp. 86-87.
3. Bird, G.A., "Monte-Carlo Simulation in an Engineering Context," Proceedings of the 12th International Symposium on Rarefied Gas Dynamics, Vol. 74, Progress in Astronautics and Aeronautics, AIAA, New York, 1981.
4. Borgnakke, Claus, and Larsen, Paul S., "Statistical Collision Model for Monte Carlo Simulation of Polyatomic Gas Mixture," Journal of Computational Physics, Vol. 18, 1975, pp. 405-420.
5. Vincenti, Walter G., and Kruger, Charles H., Jr., Introduction to Physical Gas Dynamics, John Wiley and Sons, 1965, pp. 348-356.
6. Shapiro, A.H., The Dynamics and Thermodynamics of Compressible Fluid Flow, the Ronald Press Co., New York, 1953, pp. 73-105.
7. Sharafudinov, R.G. and Skovorodko, P.A., "Rotational Level Population Kinetics in Nitrogen Freejets," Proceedings of the 12th international Symposium on Rarefied Gas Dynamics, AIAA Press 1980.
8. Bird, G.A., "Breakdown of Continuum Flow in Freejets and Rocket Plumes," Proceedings of the 12th International Symposium on Rarefied Gas Dynamics, AIAA Press, 1980.
9. Labowski, M., Ryali, S., and Fenn, J.B., "Flowfield Calculations in Nonequilibrium Freejets by the Method of Characteristics," Proceedings of the 12th International Symposium on Rarefied Gas Dynamics, AIAA Press, 1980.
10. Bird, G.A., "Breakdown of Translational and Rotational Equilibrium in Gaseous Expansions," AIAA Journal, Vol. 8, No. 11, November 1970, pp. 1997-2003.
11. Liepmann, H.W., "Gaskinetics and Gasdynamics of Orifice Flow," Journal of Fluid Mechanics, Vol. 10, No. 5, 1961, pp. 65-79.

12. Smetana, F.O., Sherrill, W.A., and Schort, D.R., "Measurements of the Discharge Characteristics of Sharp-edged and Rounded Orifices in the Transition Regime," Proceedings of the 5'th Rarefied Gas Dynamics Symposium, Vol. 2, Academic Press, 1967.

**END**

**FILMED**

**6-83**

**DTIC**